Coordination Chemistry Reviews 253 (2009) 1439–1457

Contents lists available at ScienceDirect

Coordination Chemistry Reviews

journal homepage: www.elsevier.com/locate/ccr

Review

Long-range electron transfer in artificial systems with d^6 and d^8 metal photosensitizers

Oliver S. Wenger*

Department of Inorganic, Analytical and Applied Chemistry, University of Geneva, 30 Quai Ernest-Ansermet, 1211 Geneva, Switzerland

Contents

ARTICLE INFO

Article history:
Received 31 July 2008
Accepted 9 October 2008
Available online 19 October 2008

ABSTRACT

This review article summarizes the research progress made since the year 2000 in the field of long-range electron transfer with synthetic systems that use d^6 or d^8 metal complexes as photosensitizers. This includes charge transfer over distances greater than 10 Å in both covalent and noncovalent donor–bridge–acceptor systems. Metal complexes of Ru(II), Os(II), Re(I), Ir(III), Ir(I), and Pt(II) are considered.

* Tel.: +41 22 379 60 51; fax: +41 22 379 60 69.
E-mail address: oliver.wenger@unige.ch.

0010-8545/$ – see front matter © 2008 Elsevier B.V. All rights reserved.
doi:10.1016/j.ccr.2008.10.010

Keywords:
Electron transfer
Charge-separation
Donor–acceptor systems
Electronic coupling
Photochemistry
Excited state
Molecular wires
Supramolecular chemistry
Artificial photosynthesis
Transient absorption spectroscopy
Transient infrared spectroscopy

1. Introduction

Long-range electron transfer plays a key role in chemistry and biology. Two particularly important processes that involve charge transfer over long distances are photosynthesis and respiration [1–3]. This has stimulated much research on both biological and artificial long-range electron transfer systems [4–15]. After all, it is unusual for chemical reactions to occur between two reactants that are separated spatially by 10 Å or more. A common approach to experimental investigations in this field has been to study redox reactions that can be triggered by light, whereby the progress of a long-range electron transfer can often be resolved temporally. Such kinetic information is of particular interest for the construction of artificial systems that emulate natural photosynthesis since to an important extent, solar energy conversion is a matter of speeding-up desired energy-storing (long-range) electron transfer and slowing-down undesired energy-wasting reactions [16]. The experimental approach of photoinducing the electron transfer between distant redox partners has been applied to both biological and synthetic systems. For instance, redox-active proteins have been equipped with transition metal complexes that serve as phototriggers for long-range electron transfer involving the protein active sites [17]. On the other hand, purely artificial donor–bridge–acceptor systems have been investigated in large numbers, for example porphyrin–quinone molecules that seek a close chemical analogy to the redox partners involved in the primary light-induced reactions of photosynthesis [18,19]. Many other systems considered functional mimics of the photosynthetic reaction center are based on transition metal complexes whereby d^6 and d^8 metal diimines play a prominent role [20]. It is on recent progress in this particular sub-area of the long-range electron transfer field that this review article will focus. More precisely this includes studies on artificial systems that make use of d^6 or d^8 metal complexes for investigation of light-triggered electron transfer proceeding over distances of at least 10 Å. Work published since the year 2000 will be reviewed. In a sense, the current article could therefore be considered an update of previously published reviews, either on long-range electron transfer in general [18,20–25], or on charge transfer over long distances involving metal complexes of ruthenium(II) [26–34], rhenium(I) [14], osmium(II) [26,30], iridium(III) [28,35], iridium(I) [36], and platinum(II) [37]. Indeed, these are the most popular inorganic sensitizers. We begin with a short introductory tutorial on basic concepts used in this review. It is kept brief intentionally since there exist already several excellent publications that give detailed surveys of fundamental aspects of photoinduced electron transfer [18,20,21,38,39].

All d^6 metal photosensitizers considered in this review are hexacoordinate, and the metal ions are practically in octahedral microsymmetry. In strict O_h symmetry, the set of five d-orbitals that are degenerate in the free metal ion splits into three essentially nonbonding degenerate t_{2g} orbitals and two degenerate antibonding orbitals with e_g symmetry (Fig. 1). These three- and two-fold degeneracies are further lifted by deviations from O_h to lower point symmetries, but this effect is neglected here for simplicity. The energetic splitting between the t_{2g}- and the e_g-orbital sets is essentially a function of both the chemical nature of the metal and its ligands. The polypyridine ligands relevant to this review exert fairly strong ligand fields. As far as the metal is concerned, the 4d and 5d electrons of second- and third-row metals have a larger spatial distribution than the 3d electrons of first-row metals. These two facts lead to a situation for octahedral $4d^6$ and $5d^6$ polypyridine complexes in which the HOMO corresponds to the metal-localized t_{2g}-orbitals, and the LUMO is an antibonding π^*-orbital that is localized on a polypyridine ligand; the ligand field is sufficiently strong for the e_g metal orbitals to lie energetically above the ligand π^* orbitals. This particular electronic structure forms the basis for the unique photoredox properties of this class of compounds: upon photoexcitation with visible light, an electron is promoted from the t_{2g} to the π^* orbital, resulting in a metal-to-ligand charge transfer (MLCT) state (Fig. 1, right) that is long-lived (>100 ns) in many cases. During this excited-state lifetime, the redox potentials of the complex are dramatically altered: the metal complexes become both better oxidants and reductants than in their electronic ground states (their reduction can now occur by hosting the additional electron in a t_{2g}-orbital instead of a higher-energy π^* orbital; conversely their oxidation occurs by removal of the excited π^* electron which is more readily abstracted than a t_{2g} electron in the ground state). The excited-state oxidation and reduction potentials are generally estimated by subtracting and adding, respectively, the energy of the electronic origin of the emissive ^{3}MLCT state (E_{00}) from the ground-state potentials:

$$E(M^+/{}^*M) = E(M^+/M) - E_{00} \quad (1)$$

$$E({}^*M/M^-) = E(M/M^-) + E_{00} \quad (2)$$

Based on these photoinduced redox potential changes, electron transfer can be phototriggered: reactions that are thermodynamically uphill from the ground state become exergonic upon light excitation. This is the principle of photosensitizing in the vast majority of systems considered in this review. Depending on the exact values of ground-state potentials and MLCT energies, a specific d^6 polypyridine photosensitizer may either be used preferably as an excited-state reductant or oxidant. The Re(I) and most of the Ir(III) systems mentioned in this review behave as excited-state acceptors, whereas the Os(II) complexes are donors. Ru(II) sensitizers can be both.

The energy level diagram in Fig. 2 illustrates the photoinduced processes that may occur upon excitation of a photoreductant, i.e., an excited-state donor: from the MLCT-excited state, a so-called charge-separated state with an oxidized donor and a reduced acceptor is thermodynamically accessible via an electron transfer process that is referred to as photoinduced charge-separation.

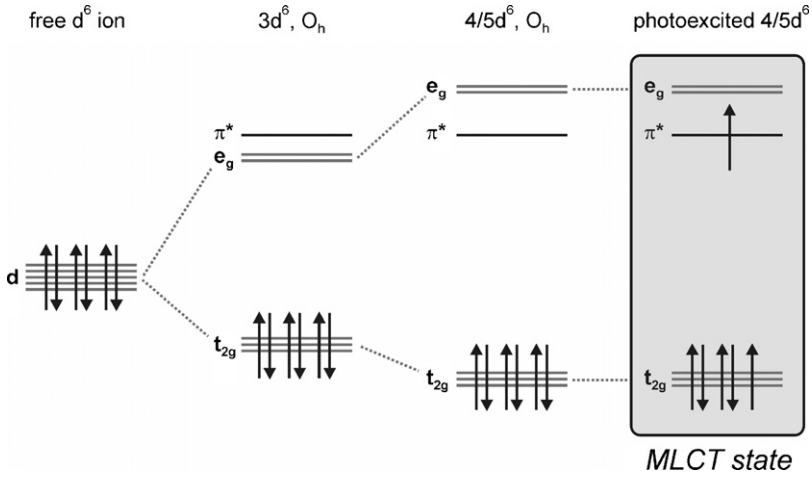

Fig. 1. Simplified molecular orbital diagram for d^6 polypyridine complexes.

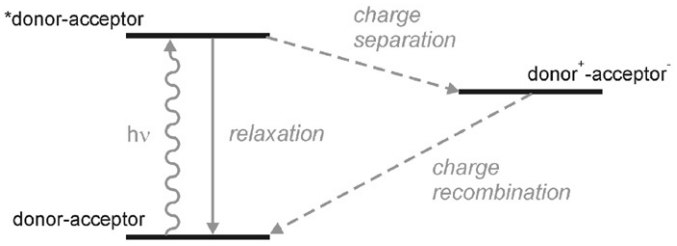

Fig. 2. Energy level diagram illustrating photoinduced charge-separation and thermal charge-recombination with a photosensitizer acting as excited-state donor.

The high-energy charge-separated state has a finite lifetime and returns back to the ground state (by any sequence of intermediate electronic states). This reverse electron transfer can occur in the absence of light and is called thermal charge-recombination. For the purpose of this review it is unimportant whether positive and negative charges are actually separated or whether the photoinduced process is merely a charge-shift; the term charge-separated state will be used even for the latter class of reactions.

If the charge-separated state is sufficiently long-lived, the light energy stored in this state can be used to drive other chemical reactions that are thermodynamically uphill [40]. This is why much contemporary research on artificial light-to-chemical energy conversion is devoted to obtaining long-lived charge-separated states. One commonly adopted strategy, encountered in many case studies presented in this review, relies on the Gaussian free energy dependence of electron transfer rates (k_{ET}):

$$k_{ET} \propto {H_{DA}}^2 \exp\left[-\frac{(\Delta G_{ET} + \lambda)^2}{4 \cdot \lambda \cdot k_B \cdot T}\right] \quad (3)$$

Eq. (3) predicts that for a given temperature T, k_{ET} will be governed by the relative magnitudes of the free energy for electron transfer (ΔG_{ET}) and the total reorganization energy (λ) associated with the charge transfer. Rates maximize for $-\Delta G_{ET} = \lambda$ because in this case the electron transfer can proceed activationless as illustrated in the middle of Fig. 3. In all other cases the charge transfer is activated and slowed down, notably also in situations where $-G_{ET}$ greatly exceeds λ. This scenario, depicted in the right part of Fig. 3, is commonly referred to as the inverted region since k_{ET} *de*creases with *in*creasing free energy in this zone. Usually, the experimentalist's aim is to tune the photoinduced charge-separation to the activationless point, whereas the thermal charge-recombinations are so exothermic that they become inverted. If this is achieved, the rate for the energy-storing process will often exceed significantly the rate for the energy-wasting thermal recombination.

A final important concept for this review is that of electronic donor–acceptor coupling, often abbreviated as H_{DA}. As seen from Eq. (3), this parameter has an important influence on electron transfer rates. H_{DA} is essentially a measure for the overlap between the redox-active orbitals from the donor with those of the acceptor, but in the long-range electron transfer systems considered here this is a bridge-mediated rather than a direct orbital overlap: so-called superexchange coupling between donor, bridge, and acceptor units is responsible for the nonzero electronic interaction in systems

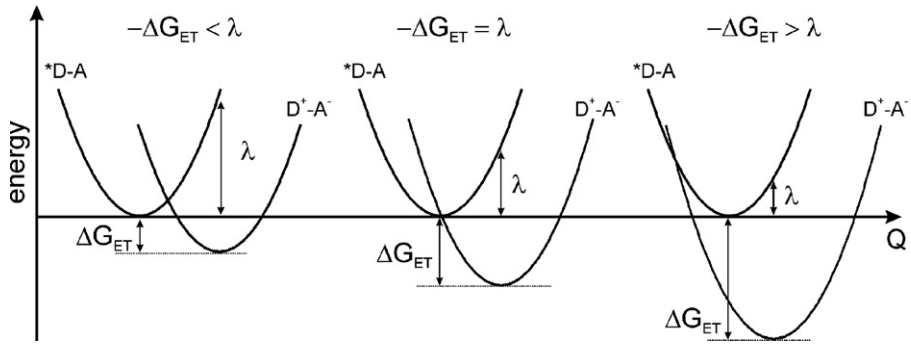

Fig. 3. Potential energy surfaces for electron transfer from a photoexcited donor (*D) to an acceptor (A) in the so-called normal, activationless, and inverted regimes. The *x*-axis (Q) is a nuclear coordinate.

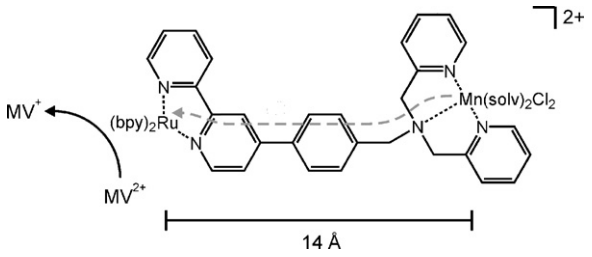

Fig. 4. Chemical structure of a Ru(II)–Mn(II) dyad. MV^{2+} stands for methylviologen. This cation is needed to generate a sufficiently oxidizing Ru(III) transient species via a bimolecular flash-quench technique [42].

with distant redox partners. This superexchange coupling usually decreases exponentially with increasing donor–acceptor distance. Charge transfer reactions that occur via this bridge-mediated superexchange mechanism are often referred to as electron tunneling or hole tunneling processes [20,21,41].

2. d^6 metal systems

2.1. Ruthenium(II) polypyridines

2.1.1. Swedish dyads and triads

Derivatives of tris(2,2'-bipyridine)ruthenium(II), $Ru(bpy)_3^{2+}$, are particularly well investigated photosensitizers for artificial photosynthetic systems [11]. In recent years, they have received continuing attention, for example in $Ru(bpy)_3^{2+}$–manganese dyads and triads that mimic the light-triggered reactions in photosystem II. Hammarström and collaborators have found that in a series of $Ru(bpy)_3^{2+}$ complexes with pendant picolylamine and aminodiacetic acid ligands similar to the one shown in Fig. 4, the ruthenium(II) ^{3}MLCT luminescence is strongly quenched upon manganese(II) complexation to these ligands: the ^{3}MLCT-excited state lifetime decreased from ~1 μs to several nanoseconds [42]. This was attributed to energy transfer involving low-lying Mn(II) ligand-field states. However, when the Ru(II)–Mn(II) distance is as long as in the molecule of Fig. 4, i.e., on the order of 14 Å, this intramolecular energy transfer quenching is less efficient, and longer Ru(II) ^{3}MLCT lifetimes (100–200 ns) result. Thermodynamically, intramolecular redox chemistry between the excited $Ru(bpy)_3^{2+}$ and the appended manganese complex is not possible, but the Ru ^{3}MLCT lifetime is now long enough for bimolecular reactions to become competitive with internal excited-state deactivation. For instance, methylviologen (MV^{2+}) can abstract an electron from the photoexcited dyads whereby a highly oxidizing Ru(III) ion is generated transiently. This in turn triggers an intramolecular Mn(II) → Ru(III) long-range electron transfer which is exothermic by 0.39–0.49 eV depending on the exact chemical nature of the dyad [43]. For donor–acceptor distances ranging from 9 to 14 Å, electron transfer rate constants between 10^5 and 2×10^7 s^{-1} were determined by means of transient absorption spectroscopy that monitored the recovery of the transiently bleached Ru(II) MLCT absorption. In view of the comparatively short donor–acceptor distances, these rates are rather slow. For comparison, driving-force optimized ($-\Delta G_{ET} \approx \lambda$) electron tunneling through 14 Å of protein backbone takes place with ~10^8 s^{-1} [21]. Temperature dependent studies performed on seven different dyads between 10 and 70 °C reveal organization energies λ of 1.5–2.0 eV associated with the intramolecular Mn(II) → Ru(III) electron transfer. These large λ-values are believed to be due to significant intramolecular rearrangements that accompany Mn(II) oxidation, and they explain why for $-\Delta G_{ET}$ = 0.39–0.49 eV the rate of Mn(II) → Ru(III) electron transfer is rather modest [43].

In another recent study the Swedish researchers from above explored a series of ruthenium(II) 2,2′-bipyridine (bpy) and 2,2′:6′,2″-terpyridine (tpy) complexes with covalently attached naphthalenediimide (NDI) acceptors [44]. The bpy complexes behave as electron transfer dyads in which a Ru(III)–NDI^- charge-separated state forms via an energy transfer intermediate, an NDI triplet excited state. The tpy complexes on the other hand showed essentially no energy or electron transfer processes which is due to the short MLCT lifetime in these species. Building on this and the prior manganese research, Hammarström and collaborators reported recently on a manganese dimer–Ru(II)–naphthalenediimide triad with an unusually long-lived charge-separated state (Fig. 5) [45]. This molecule is essentially a $Ru(bpy)_3^{2+}$ complex with two NDI substituted bpy ligands and a third bpy ligand that bears a binuclear manganese(II) complex. A combination of time-resolved optical spectroscopic and EPR techniques proved necessary to elucidate fully the

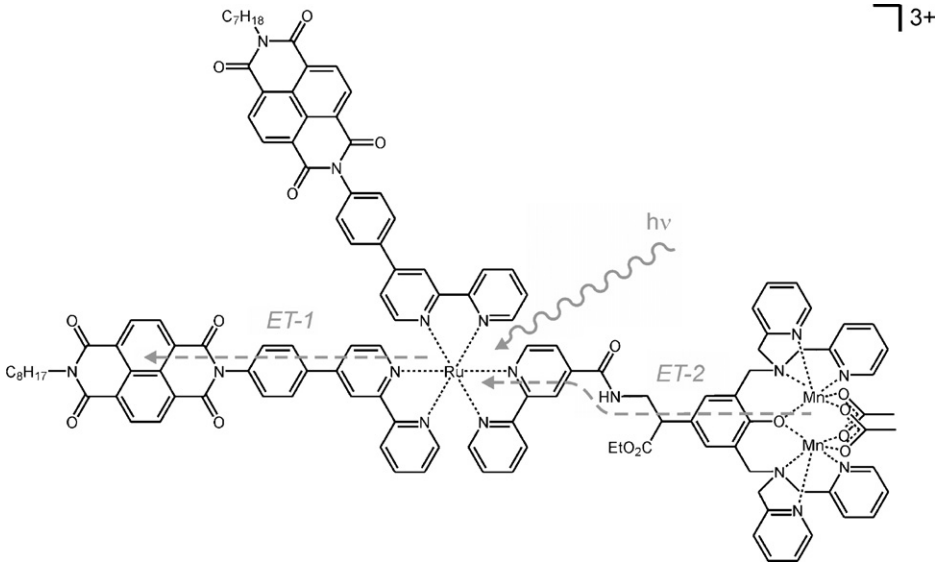

Fig. 5. Triad based on a binuclear Mn(II)/Mn(II) donor, a ruthenium(II) photosensitizer, and a naphthalenediimide (NDI) terminal acceptor [45].

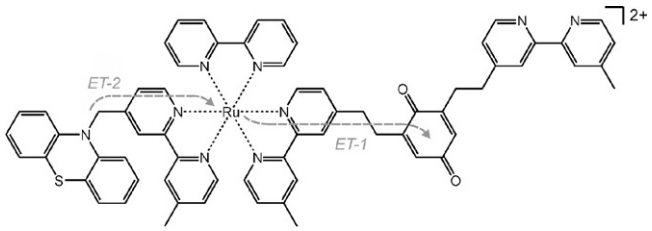

Fig. 6. A triad for phototriggered phenothiazine-to-benzoquinone electron transfer [49].

photoinduced processes that occur in this system. As in the abovementioned $Ru(bpy)_3^{2+}$–NDI dyads, the primary process is an electron transfer from the photoexcited metal center to the NDI (marked ET-1 in Fig. 5) whereby an NDI radical anion is formed. By contrast to the abovementioned dyads, in this triad one does not observe a Ru(III) intermediate as an oxidation product. This is because a charge-shift from the Mn(II)/Mn(II) dimer to the oxidized ruthenium takes place within less than 30 ns, thereby generating a Mn(II)/Mn(III)–Ru(II)–NDI^- charge-separated state with a lifetime of 600 μs in room temperature solution. The unusual stability of this state is again attributed to the very large (internal) reorganization energy ($\lambda \approx 2.0$ eV) that is associated with charge-recombination; this is due to important differences in metal-to-ligand bond lengths (~0.2 Å) when the manganese complex changes its oxidation state from Mn(II)/Mn(II) to Mn(II)/Mn(III). In fluid butyronitrile at 140 K, this strongly activated ($-\Delta G_{ET} \approx 1.1$ eV) intramolecular charge-recombination occurred on a 0.1–1 s timescale.

When the triad from Fig. 5 is prepared without the manganese ions, i.e., with the free picolylamine ligand, a molecule suitable for proton-coupled electron transfer studies is obtained (not shown) [46]. The free ligand contains a hydrogen bonded phenol that can act as an electron donor to photogenerated $Ru(bpy)_3^{3+}$ (the initial Ru(II) complex is photooxidized by a covalently attached NDI acceptor), whereby the phenolic proton is released. The same picolylamine ligand can also form complexes with ruthenium. This yields a mixed-valent Ru(II)/Ru(III) moiety that can be covalently linked to a $Ru(bpy)_3^{2+}$ photosensitizer as in the manganese triad from Fig. 5 [47]. One of the original aims of this mixed-valent ruthenium dyad work was to improve the water oxidation capability of previously investigated dinuclear ruthenium complexes [48]. However, the new dyad proved to be more useful as a photosensitizer on a nanocrystalline TiO_2 surface.

Fig. 6 shows a phenothiazine (PTZ)–$Ru(bpy)_3^{2+}$–benzoquinone (BQ) triad that was investigated recently by the teams around Hammarström, Åkermark, and Sun. When the ruthenium(II) complex is photoexcited, a PTZ^+–BQ^- charge-separated state forms via a sequence of Ru(II) → BQ and PTZ → Ru(III) electron transfer steps [49]. The final charge-separated state forms with unusually high yield (>90%), is fairly long-lived (80 ns), and stores a significant amount of energy (1.32 eV). Unfortunately the molecule turned out to be photolabile, and the original plan, namely to prepare a tetrad by attaching a terminal electron acceptor at the pendant bpy ligand, failed.

The same laboratories report on a triad comprised of a cyclometalated ruthenium(II) complex, a $Ru(bpy)_3^{2+}$ unit, and a pyromellitimide acceptor (not shown) [50]. This triad works as a combined antenna/charge-separation system, but fails to exhibit distant charge-separation through sequential absorption of two photons as attempted to observe via pump-pump-probe experiments. Such multicomponent molecular species containing both an antenna and a charge-separation subunit are still relatively rare [51–53].

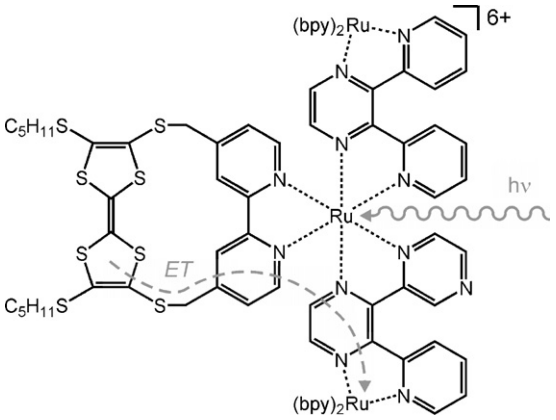

Fig. 7. Trinuclear ruthenium(II) complex with an appended tetrathiafulvalene (TTF) unit. Photoexcitation of the central ruthenium leads to electron transfer from the TTF to a peripheral Ru complex [54].

2.1.2. Reductive excited-state quenching with tetrathiafulvalene donors

In recent years, tetrathiafulvalene (TTF) donors have also received some attention in conjunction with $Ru(bpy)_3^{2+}$ photosensitizers. A case in point is the trinuclear Ru(II) complex with a TTF moiety covalently attached to a bpy ligand in Fig. 7 [54]. In this system photoexcitation of the trinuclear ruthenium core very rapidly (<200 fs) leads to the selective formation of an MLCT-excited state involving a *peripheral* ruthenium and a 2,3-bis(2′-pyridyl)pyrazine (dpp) bridging ligand. This is followed by a long-range electron transfer from the TTF via the *central* ruthenium(II) to the MLCT-excited *peripheral* ruthenium. This reaction sequence was inferred from a variety of careful control experiments on a series of suitable reference molecules. The failure to observe the oxidized TTF in transient absorption experiments was explained by a charge-recombination rate that is higher than the rate for charge-separation. This makes sense because the forward process can be expected to benefit from stronger electronic coupling than the backward reaction: charge-separation involves two more distant subunits (the TTF and a peripheral Ru center), whereas charge-recombination occurs from a dpp bridging ligand to the oxidized TTF, i.e., over a somewhat shorter distance. As a consequence, a significant population of the charge-separated state never builds up, and the TTF^+ radical cation cannot be observed.

An intriguing TTF–$Ru(bpy)_3^{2+}$ donor–acceptor system has been explored by Decurtins, Hauser and their research groups [55,56]. In synthetically very challenging work, they fused a TTF molecule onto the back of a dipyridophenazine (dppz) ligand that was complexed to a ruthenium(II) to give either the homoleptic tris-complex or heteroleptic complexes with bpy auxiliary ligands (Fig. 8). In the homoleptic tris-TTF–dppz molecule, ^{1}MLCT excitation leads to a long-lived energy-rich state (2.3 μs in CH_2Cl_2 at room temperature) in which a positive and a negative charge are located on two differ-

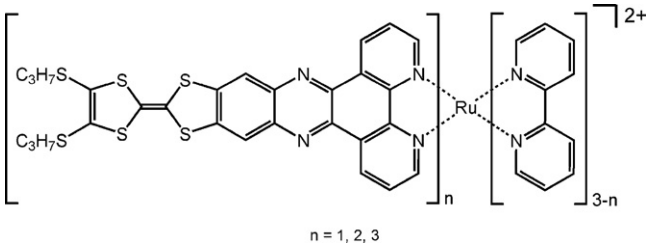

Fig. 8. Ru(II) tris(α-diimine) complexes with a tetrathiafulvalene (TTF) donor fused onto the back of a dipyridophenazine (dppz) ligand [55,56].

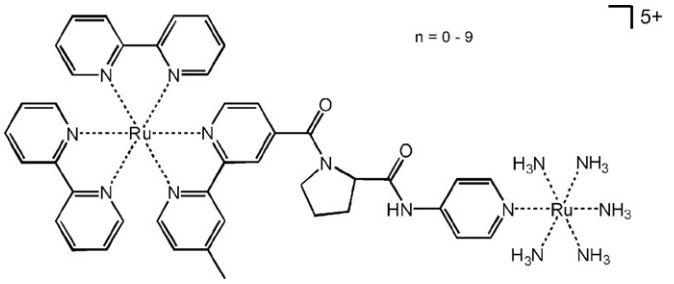

Fig. 9. Dyads for the study of long-range electron tunneling across oligo-proline bridges of variable lengths [58].

ent TTF–dppz ligands. Direct evidence for this comes from transient absorption experiments in which the spectroscopic fingerprint of a TTF^+ radical cation attached to a charge-neutral dppz is observed at the same time with the spectroscopic signature of an isolated $dppz^-$ radical anion. In the heteroleptic complex with $n = 2$ the same charge-separated state forms, but for the system with $n = 1$, a different behavior is observed: due to the lack of a separate dppz acceptor for the electron coming from the TTF donor, the electron acceptor in this case is one of the bpy auxiliary ligands. However, this bpy^-–Ru(II)–dppz–TTF^+ charge-separated state forms only very inefficiently from the initially excited bpy–Ru(III)–$dppz^-$–TTF MLCT state. This is likely due to the fact that electron tunneling from the TTF to the ruthenium(III) is now associated with a large Coulomb barrier that is caused by the dppz-localized electron. Thus, the initially excited MLCT state not only relaxes to a long-range charge-separated state but in part also to a luminescent ^{3}MLCT state.

2.1.3. Systems with long helicoidal and rigid rod-like bridges

Two recent studies make use of the $Ru(bpy)_3^{2+}$ photosensitizer as a tool for mechanistic investigations of long-range electron transfer in oligo-proline bridged systems. The group of T.J. Meyer attached phenothiazine donors and ruthenium(II) complexes via amide bonds to helical oligo-proline assemblies comprised of 16–19 proline residues (not shown) [57]. The striking observation is that PTZ → *Ru(II) electron transfer rates correlate with the through-space donor–acceptor distances (rather than the through-bond distances) in the four dyads investigated. This implies that in these helical oligo-prolines, the through-bond electron transfer is less important. By contrast, Isied, Wishart and coworkers find long-range electron transfer through their donor–acceptor substituted oligo-prolines to occur via a through-bond mechanism [58]. They measured the rates for $Ru(bpy)_3^{2+} \rightarrow [Ru(NH_3)_5]^{3+}$ electron transfer in 10 dyads in which the number of intervening proline units increased from 0 to 9, Fig. 9. A combination of photolysis and radiolysis methods was necessary because starting with $n = 5$, the $Ru(bpy)_3^{2+}$ excited-state lifetime is too short for electron transfer quenching to be a competitive excited-state deactivation pathway. Interestingly the distance dependence of electron transfer rates revealed the presence of two different regimes: for the shorter peptides ($n = 0$–4) a strong distance dependence ($\beta = 1.4$ Å^{-1}) was found whereas for the longer systems ($n = 5$–9) a much weaker rate attenuation was observed with increasing distance ($\beta = 0.18$ Å^{-1}). This was interpreted in terms of a changeover from a relatively inefficient superexchange tunneling to a more efficient hopping mechanism.

E. Galoppini, G.J. Meyer, and coworkers explored the long-range electron transfer from $Ru(bpy)_3^{2+}$ photosensitizers to nanocrystalline TiO_2 surfaces via phenylethynyl bridging units [59]. Four phenyladamantane tripods such as the one shown in Fig. 10 were investigated. The rigid tripodal design should ensure a stable, well-defined three-point attachment to the surface of the metal oxide nanoparticles. The motivation for this work came from the insight that even if $Ru(bpy)_3^{2+} \rightarrow TiO_2$ charge-injection rates were 3–4 orders of magnitude slower than for $Ru(bpy)_3^{2+}$ photosensitizers that are attached directly to a TiO_2 surface (i.e., via carboxylate groups at the 4- and 4′-positions of one or several bpy ligands), the charge-injection efficiency could still be expected to be near unity while the reverse back electron transfer may be slowed down significantly. Through increase of the Ru–TiO_2 distance it might thus be possible to get better discrimination between charge-injection and charge-recombination efficiencies. In the investigated systems the Ru–TiO_2 distance is ~17 Å, and indeed a charge-injection efficiency near unity was inferred from time-resolved optical spectroscopic measurements. Disappointingly, the charge-recombination rates were found to be equally high as in the complexes mentioned above with much shorter Ru–TiO_2 distances. Despite the careful design, it is not absolutely clear whether these molecules really stand up from the surface. It is therefore possible that charge-recombination occurs via a (shorter) through-space rather than the 17 Å through-bond pathway.

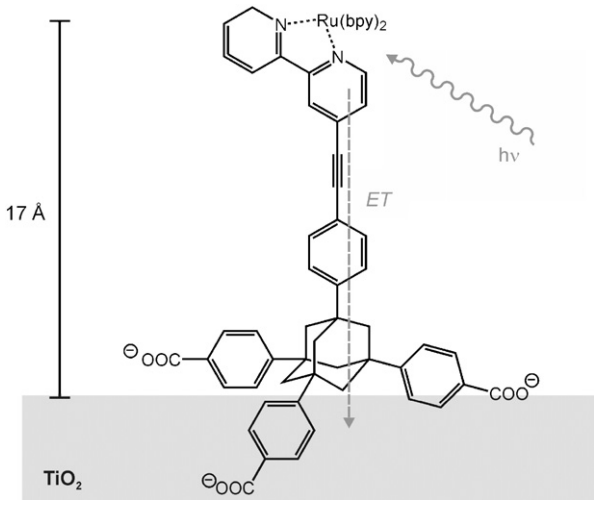

Fig. 10. Tripodal photosensitizer for charge-injection into nanocrystalline TiO_2 [59].

2.1.4. Supramolecular systems involving charge transfer across noncovalent bonds

The $Ru(bpy)_3^{2+}$ complex has also been useful for electron transfer studies in supramolecular systems. König, De Cola and coworkers investigated reductive quenching of the $Ru(bpy)_3^{2+}$ ^{3}MLCT state by *N*,*N*,*N*′,*N*′-tetramethyl-*p*-phenylenediamine (TMPD) whereby acceptor and donor were held together by a $Sc(acac)_3$ (acac = acetylacetonate) structural motif, Fig. 11 [60]. This scandium complex is redox inactive but kinetically labile, i.e., a mixture of donor–acceptor assemblies with different stoichiometries forms and the molecule shown in Fig. 11 is only one example out of many different ones that are present in solution. The average (room-temperature) lifetime of these individual Sc(III) complexes is about 5 μs and thus, in their excited states, the individual donor–acceptor (supra)molecules can be considered as static species. The rate constant for TMPD → *Ru(II) electron transfer in the Sc(III) complex from Fig. 11 is 9×10^8 s^{-1} based on time-resolved luminescence experiments. The reverse process, i.e., Ru(I) → $TMPD^+$ electron transfer proceeds with 2.4×10^7 s^{-1} based on transient absorption data. Importantly, in absence of Sc(III) ions, no electron transfer at all is observed under the very dilute conditions (conc. ~10^{-5} M) i.e., bimolecular electron transfer is negligible.

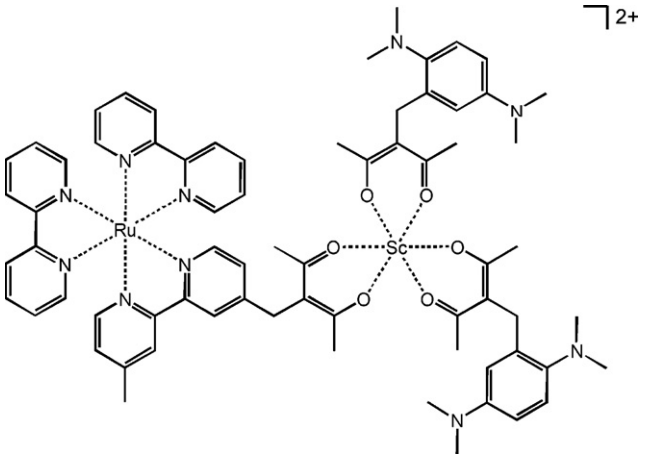

Fig. 11. A kinetically labile assembly comprised of *N*,*N*,*N*′,*N*′-tetramethyl-*p*-phenylenediamine (TMPD) donors and a $Ru(bpy)_3^{2+}$ acceptor [60].

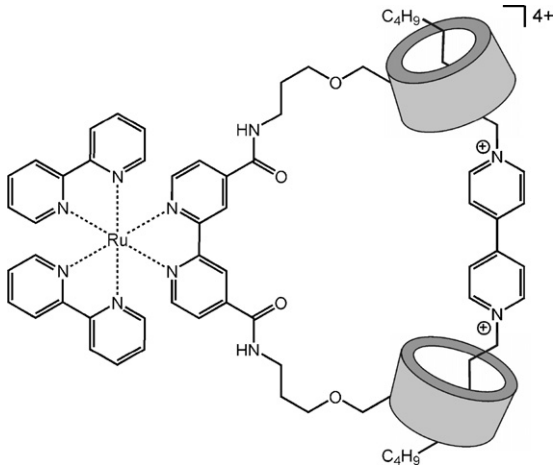

Fig. 12. A supramolecular donor–acceptor dyad based on hydrophobic interactions between the long alkyl-chains of a viologen electron acceptor and the cavity interior of β-cyclodextrins [61].

Another recent example of a supramolecular long-range electron transfer involves a $Ru(bpy)_3^{2+}$ complex with β-cyclodextrin units attached to the backbone of one bpy ligand, Fig. 12 [61]. Under the condition that sufficiently long alkyl chains are used, *N*,*N*′-dialkyl substituted 4,4′-bipyridinium ions form supramolecular assemblies with these cyclodextrin containing complexes. Binding constants in pH-neutral water are of the order of $10^4\ M^{-1}$ for an *N*,*N*′-dinonyl-4,4′-bipyridinium. The electron transfer from the photoexcited ruthenium complex to the viologen acceptor takes place with a rate constant of $4.3 \times 10^7\ s^{-1}$. Surprisingly, the singly reduced viologen species escaped detection. This is likely due to the rapidity of the electron transfer process in the reverse direction.

In prior work, the Pikramenou group, partially in collaboration with the De Cola team, investigated supramolecular electron (and energy) transfer in similar metallocyclodextrin systems [62–64]. One of these (Fig. 13) is comprised of a ruthenium(II) bis((4′-tolyl)-2,2′:6′,2″-terpyridine) complex, $Ru(ttpy)_2^{2+}$, that is attached covalently to the rim of a β-cyclodextrin. The latter was methylated to obtain good solubility of the overall complex in both aqueous (for binding studies to hydrophobic guests) and organic solvents (for sample purification). A biphenyl-substituted osmium bis(tolylterpyridine) complex forms 1:1 adducts with the metallocyclodextrin receptor; the hydrophobic interactions between the biphenyl and the cyclodextrin cavity interior turned out to be particularly strong in buffered aqueous solutions with high ionic strengths. The initial oxidation state of the osmium is +II, but it can easily be oxidized to +III using a cerium(IV) oxidant. The resulting Ru(II)–Os(III) dyad (Fig. 13) is stable, and photoexcitation of the ruthenium complex now induces a Ru(II)-to-Os(III) electron transfer. This manifests itself in a biphasic Ru ^{3}MLCT luminescence decay with a slow (τ = 1.9 ns) and a dominant (80%) fast (τ = 100 ps) component. The former matches the ^{3}MLCT-excited state lifetime of the unsubstituted $Ru(ttpy)_2^{2+}$ reference complex and is assigned to guest-free metallocyclodextrin, whereas the latter is attributed to the abovementioned electron transfer process in supramolecular 1:1 donor–acceptor adducts. The rate constant for the supramolecular electron transfer has been estimated to be $9.5 \times 10^9\ s^{-1}$; this large value has been explained in terms of the very high exothermicity ($-\Delta G_{ET} \approx 1.6$ eV) of the process.

2.1.5. Intervalence long-range electron transfer in ruthenium dimers

The molecules discussed in this sub-paragraph are examples of direct optical metal-to-metal electron transfer in strongly coupled molecules as opposed to photoinduced (and therefore stepwise) processes in weakly coupled donor–acceptor systems. They are thus fundamentally different from all other systems discussed in this review.

Ruthenium has traditionally played a key role in intervalence electron transfer research. There exist several examples for which an intervalence charge transfer involves Ru(II) and Ru(III) centers that are separated by more than 10 Å [65]. A particularly intriguing recent study reports on a Class III mixed-valence Ru(II)/Ru(III) system in which the metal centers are 19.5 Å apart, Fig. 14 [66]. The bridging ligand between them is 4,4′-azodi(phenylcyanamide), and each metal center has one tpy and one bpy auxiliary ligand. Cyclic voltammetry experiments lead to the conclusion that the comproportionation equilibrium constant for this complex is of the order of 10^{13}, implying very strong metal–metal coupling despite their

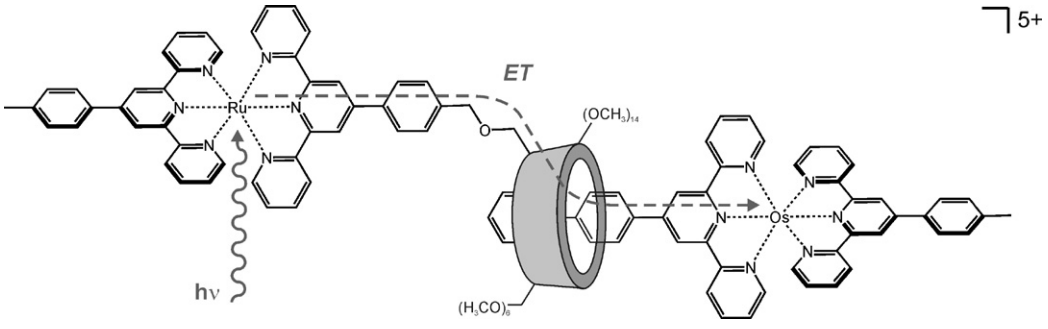

Fig. 13. Supramolecular Ru(II)–Os(III) dyad [62,64].

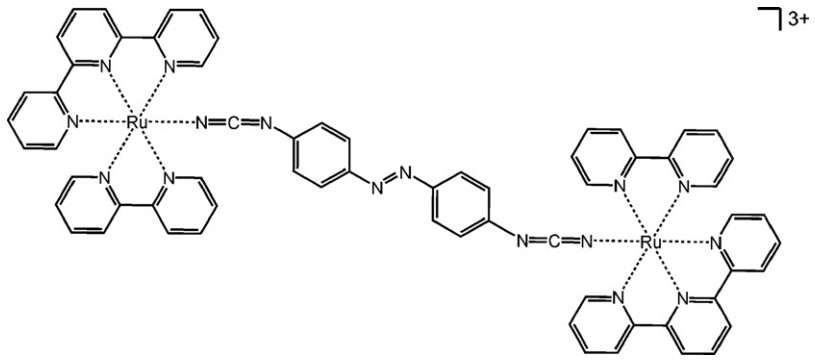

Fig. 14. A mixed-valent Ru(II)–Ru(III) system in which long-range intervalence charge transfer takes place very efficiently [66].

large separation from one another. Optical absorption spectroscopy reveals an absorption band centered around 1920 nm which is only observed for the mixed-valent species. Consequently it has been attributed to an intervalence transition, and its analysis yields a metal–metal electronic coupling of ~2600 cm^{-1}. This is lower than what would be predicted based on the comproportionation constant, but is not contradictory considering that the redox potential split in the cyclic voltammogram is likely due to both intermetallic electronic coupling and electrostatic effects. At any rate, the extraordinarily strong metal–metal coupling in the system of Fig. 14 has been explained by the capability of the bridging ligand to mediate superexchange very efficiently via both its HOMO and LUMO: both orbitals have the correct symmetry to interact simultaneously with the relevant ruthenium orbitals, and the HOMO–LUMO energy gap is only 1.07 eV.

In a related study the groups of Harriman and Ziessel reported on ethynylene-coupled bis(terpyridine) complexes of ruthenium (not shown) [67]. In these mixed-valent complexes, metal–metal coupling is very weak, but extensive electron delocalization occurs upon one-electron reduction. This is because the bridging molecules have very large LUMOs that extend over most of these ligands.

2.2. Rhenium(I) tricarbonyl diimines

2.2.1. Studies using transient infrared spectroscopy

Rhenium(I) tricarbonyl diimines are frequently used for phototriggered electron transfer studies. With their most intense absorptions located in the blue and UV spectroscopic ranges, these complexes are much poorer light harvesters than $Ru(bpy)_3^{2+}$, but in their long-lived excited states the rhenium(I) tricarbonyl diimines are usually significantly more potent oxidants. Perutz and collaborators reported on $Re(bpy)(CO)_3$–metalloporphyrin dyads, Fig. 15, which provide illustrative examples of supramolecular photochemical systems [68,69]. Visible light irradiation (>495 nm) of these dyads selectively excites the porphyrin moiety, thereby triggering a long-range electron transfer from the zinc(II) porphyrin to the rhenium complex. This in turn leads to the expulsion of an axial 3-methylpyridine ligand coordinated to the rhenium. In presence of bromide ions, the corresponding bromo-complex ($L = Br^-$; $n = 0$) forms quantitatively after ligand substitution and back electron transfer from the reduced rhenium to the oxidized porphyrin [68]. The porphyrin part of the dyad has the dominant optical absorption features, and therefore UV–vis transient absorption spectroscopy is not suitable for the investigation of the photoredox processes that occur on the rhenium moiety. Instead, transient infrared spectroscopy was employed, whereby elegant use of the CO stretching frequencies as spectroscopic handles was made [69]. Porphyrin → $Re(bpy)(CO)_3$ electron transfer causes a 20–30 cm^{-1} red-shift of these IR absorptions due to increased Re-to-CO π-backbonding. These experiments reveal that for the Zn(II) porphyrin from Fig. 15 the intramolecular electron transfer from the photoexcited porphyrin to the rhenium occurs with a time constant of 5 ps. The resulting charge-separated state has a lifetime of only 40 ps and relaxes to a vibrationally excited electronic ground state. Relaxation of this vibrationally hot state takes another 35–55 ps.

A combination of transient absorption, time-resolved resonance Raman, and time-resolved IR spectroscopy was employed to investigate the photoinduced processes occurring in the triad shown in Fig. 16 [70]. UV excitation of this molecule leads to the formation of a relatively long-lived (300 ns) charge-separated state: transient absorption provides clear evidence for the phenothiazine radical cation and for the anthraquinone radical anion. Transient IR experiments further confirm the formation of the latter (the quinone-based CO stretch shifts by −118 cm^{-1}), and, importantly, they show that the electron density at the rhenium complex is rel-

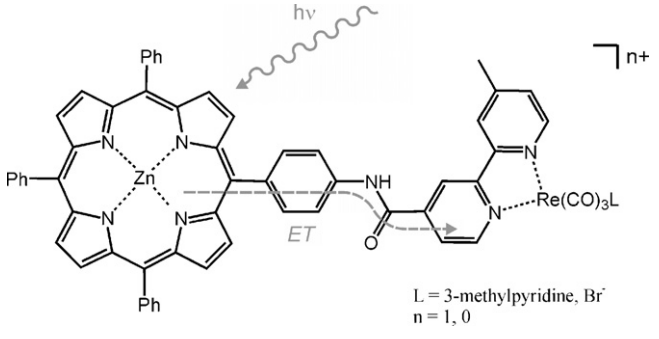

Fig. 15. Zinc(II) porphyrin–rhenium(I) dyad that has been investigated by transient IR spectroscopy [68,69].

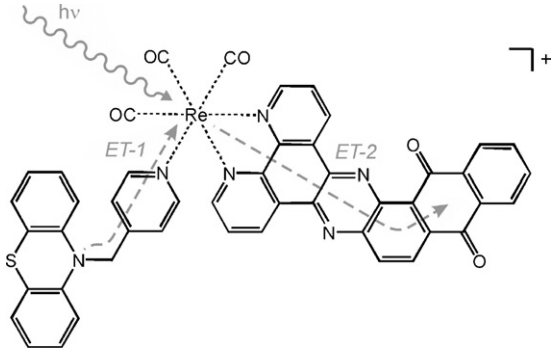

Fig. 16. Triad based on a phenothiazine donor, a rhenium(I) tricarbonyl diimine photosensitizer, and an anthraquinone acceptor [70].

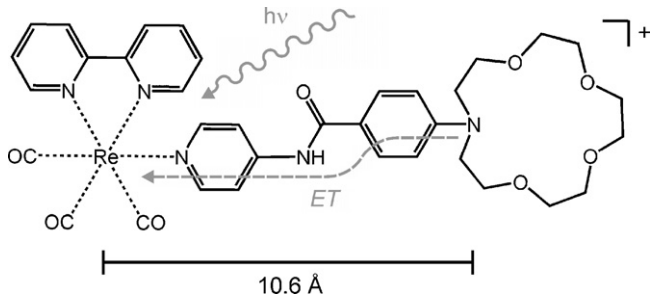

Fig. 17. Azacrown–rhenium(I) dyad for light-triggered cation release [71].

atively unperturbed compared to the ground state (the IR bands of the metal bound carbonyls shift by less than $-15\,cm^{-1}$). In other words, the rhenium stays formally in the +I oxidation state. The slow rate of back electron transfer from the reduced anthraquinone to the oxidized phenothiazine has been explained in terms of weak electronic coupling between the two moieties due to the presence of orbital nodes at the connecting metal center.

2.2.2. Towards electron transfer-triggered cation release from an azacrown

The photoreactivity of a rhenium(I) tricarbonyl 2,2′-bipyridine complex with a covalently attached azacrown, Fig. 17, could be elucidated fully by time-resolved UV–vis spectroscopy [71]. In this molecule the tertiary amine acts as an electron donor and the photoexcited metal complex is the electron acceptor; the through-bond donor–acceptor distance is 10.6 Å. The intramolecular charge transfer occurs with a time constant of 0.5 ns whereby a so-called ligand-to-ligand charge transfer (LLCT) state forms: the bpy ligand bears a negative, the azacrown a positive charge. Protonation of the azacrown raises the energy of this state above the ^{3}MLCT level, and electron transfer is suppressed for thermodynamic reasons. This manifests itself in an increase of the luminescence lifetime from <1 ns to 138 ns and a concomitant increase of the luminescence intensity. Transient absorption experiments show that charge-recombination is a factor of 38 slower than charge-separation. Two explanations are given for this observation: (i) forward electron transfer is moderately exergonic ($\Delta G_{ET} = -0.14$ eV) and occurs in the Marcus normal region (the estimated total reorganization energy λ is 1.0 eV) whereas back electron transfer is highly exergonic ($\Delta G_{ET} = -2.29$ eV) and occurs in the Marcus inverted region; (ii) the forward electron transfer occurs over a shorter distance (from the azacrown to the rhenium(II) center) than back electron transfer (from the bpy ligand to the azacrown), i.e., electronic donor–acceptor coupling is weaker for the charge-recombination than for the charge-separation. The azacrown–rhenium donor–acceptor molecule in Fig. 17 may be of interest for light-triggered cation release: azacrowns can bind small cations; upon electron transfer a radical cation forms at the nitrogen atom which may be expected to lead to expulsion of such a cationic guest.

2.2.3. Supramolecular dyads formed by hydrogen bonding or hydrophobic interactions

Rhenium(I) tricarbonyl diimines have also been useful for exploring long-range electron transfer in self-assembled donor–acceptor systems. A case in point is the barbiturate-based host–guest system shown in Fig. 18 [72] comprised of a luminescent rhenium(I) complex with a 2,2′-bipyridine ligand that has a covalently attached barbiturate. This entity forms relatively stable 1:1 adducts with a barbiturate receptor bearing a methylviologen unit on its back. In dichloromethane the association constant K_a

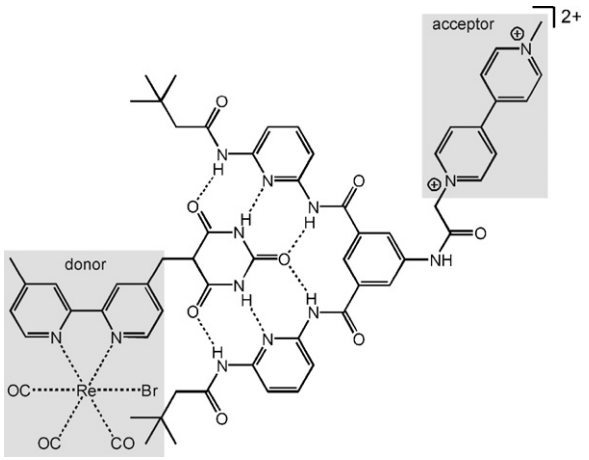

Fig. 18. A supramolecular donor–acceptor system that assembles due to the hydrogen bonding between a barbiturate and an appropriate receptor [72].

is $2 \times 10^5\,M^{-1}$ (based on ^{1}H NMR titrations), thanks to the formation of six hydrogen bonds between the host and the guest. The formation of these supramolecules manifests itself also in DOSY experiments that reveal a significant decrease in the diffusion coefficient as a result of the adduct formation. The luminescence of the rhenium complex is strongly quenched upon binding to the barbiturate receptor; the ^{3}MLCT lifetime decreases from 60 ns to less than 3 ns. This is due to electron transfer from the metal complex to the methylviologen which is exergonic by 0.43 eV; the formation of the methylviologen radical cation is corroborated by transient absorption spectroscopy. As in the abovementioned covalent rhenium(I) dyads, the back electron transfer from the reduced acceptor (the methylviologen) to the oxidized donor (the rhenium complex) is significantly slower (~4 orders of magnitude) than the forward electron transfer. In analogy to the prior studies, this has been attributed to an inverted driving-force effect. The striking observation of this study is the rapidity of the forward electron transfer: the methylviologen radical forms on a sub-picosecond timescale which is surprisingly fast considering the relatively long donor–acceptor separation distance. As a possible explanation, De Cola and coworkers invoke electron transfer from the initially populated ^{1}MLCT, before relaxation to the corresponding triplet state occurs. The driving-force for electron transfer from the singlet excited state is expected to be higher than from the triplet state, which may explain the faster-than-usual charge transfer rate. The possibility of a through-solvent electron tunneling process in a special conformer of the donor–acceptor adducts has also been discussed. It is possible that the electron transfer occurs preferentially when the rhenium(I) complex and the methylviologen find themselves on the same side of the plane formed by the barbiturate entity and its receptor. There is enough conformational freedom for the donor and the acceptor to come almost into contact with one another. In this scenario, the electron transfer would not occur across the hydrogen bonds of the barbiturate core but across van der Waals gaps. This ambiguity regarding the exact electron transfer mechanism underscores the usefulness of rigid donor–bridge–acceptor systems for in-depth mechanistic studies.

Another recent example of a supramolecular long-range electron transfer involving rhenium(I) complexes is provided by the β-cyclodextrin–fullerene adduct systems shown in Fig. 19 [73]. The formation of these supramolecules is based on hydrophobic interactions between the cavity interior of the cyclic oligo-saccharides and the C_{60} molecules. The diameter of the fullerene (~1.0 nm) exceeds the size of the inner diameter of the β-cyclodextrin

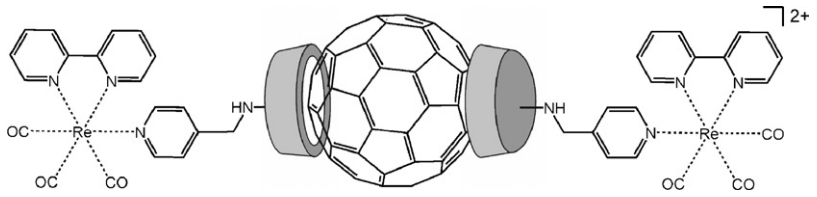

Fig. 19. A rhenium–fullerene–rhenium system held together tightly by the hydrophobic interactions between β-cyclodextrins and the C_{60} molecule [73].

(~0.57 nm) and therefore complete C_{60} inclusion is not possible. Instead, a 2:1 cyclodextrin/C_{60} adduct forms when appropriate molar quantities of the individual components are refluxed in a DMF/toluene solvent mixture for two days. Evidently, these adducts only form under conditions that are much more forcing than those needed for the formation of the cyclodextrin-methylviologen and cyclodextrin-biphenyl assemblies from Figs. 12 and 13. However, once the supramolecules in Fig. 19 are formed, they are remarkably stable. Upon photoexcitation of the rhenium(I) complex, its emissive ^{3}MLCT-excited state is quenched with a time constant of 14 ns which has been attributed tentatively to a strongly exergonic ($\Delta G_{ET} = -1.0$ eV) *rhenium(I) → fullerene electron transfer process. Based on thermodynamic grounds, energy transfer cannot be fully excluded as a possible excited-state quenching process in this system, and the authors point out the necessity of transient absorption experiments in order to understand completely the photoreactivity of these supramolecules [73].

2.2.4. Distance-dependence studies of charge tunneling

The Wenger group has used rhenium(I) tricarbonyl 1,10-phenanthroline (phen) complexes for phototriggered long-range electron tunneling through oligo-*p*-xylene bridges, Fig. 20 [74]. The peculiarity of these rigid conjugated bridges is that they have essentially length-independent HOMO–LUMO energy gaps which is in clear contrast to oligo-*p*-phenylene bridges that lack methyl-substituents. This is illustrated by the two series of optical absorption spectra in Fig. 20, each showing the spectra of four homologous donor–bridge–acceptor molecules: mono- to tetra-*p*-phenylene bridged dyads on the left, and mono- to tetra-*p*-xylene bridged dyads on the right. The difference between the two data sets is striking. The spectra of the four xylene bridged dyads on the right are practically superimposable onto one another but with increasing number of unsubstituted phenyl bridging units (on the left) there is a pronounced red-shift of some of the UV bands. Using time-resolved luminescence and transient absorption spectroscopy, it has been possible to extract electron tunneling rates k_{ET} for four *p*-xylene bridged systems, ranging from a molecule with a donor–acceptor separation r_{DA} of 10.6 Å (with a bi-*p*-xylene bridge) for which $k_{ET} = 5 \times 10^7$ s^{-1} to a penta-*p*-xylene bridged dyad with $r_{DA} = 27.9$ Å and $k_{ET} = 8 \times 10^4$ s^{-1}. From these data it is possible to extract a distance decay parameter β for the long-range electron tunneling process from the phenothiazine to the photoexcited rhenium complex. The numerical value for β is 0.52 Å^{-1}, which is strikingly close to β-values reported previously for unsubstituted phenylene spacers [75–78]. Thus, the oligo-*p*-xylene bridges can mediate electron tunneling almost equally well as oligo-*p*-phenylenes, despite the higher degree of π-conjugation in the latter [74].

Conformational effects on long-range electron transfer across oligo-*p*-phenylene bridges have also been investigated recently by Indelli, Scandola, and coworkers [78]. Specifically, they studied phototriggered Ru(II)-to-Rh(III) electron transfer in dyads with up to three phenyl bridging units between the ruthenium and rhodium polypyridine complexes (not shown). Interestingly, the 24 Å electron tunneling step across an unsubstituted tri-*p*-phenyl spacer was about an order of magnitude faster than in an analogous tri-*p*-phenyl-bridged dyad in which the central phenyl unit bears two *n*-hexyl chains. This has been explained by a decrease in bridge-mediated electronic donor–acceptor coupling as the hexyl-substituents demand a larger inter-phenyl torsion angle. In other words, superexchange coupling becomes less efficient upon bridge substitution. In the Ru(II)–triphenyl–Rh(III) systems an increase in the torsion angle from 45° to 75° between the central phenyl and the two adjacent phenyl units would be sufficient to account for

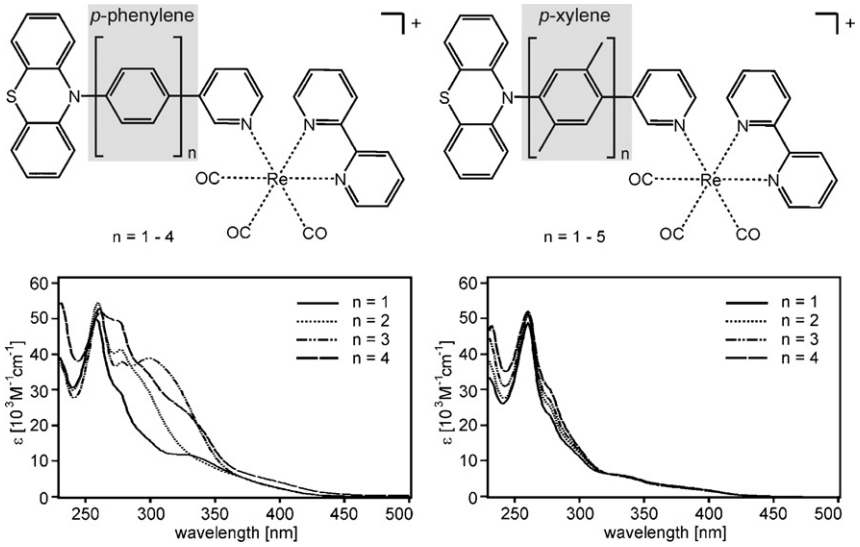

Fig. 20. Comparison of oligo-*p*-phenylene and oligo-*p*-xylene bridges in phenothiazine–rhenium(I) donor–acceptor dyads. The optical absorption spectra show that the xylene bridges on the right have essentially length-independent HOMO–LUMO energy gaps—contrary to the phenylene systems on the left [74].

the experimentally observed decrease of the electron transfer rate upon hexyl-substitution of that central spacer [20].

2.3. Osmium(II) polypyridines

2.3.1. French-Italian bis-tolylterpyridine systems

The $Os(bpy)_3^{2+}$ complex is much less frequently chosen as a photosensitizer than the isoelectronic $Ru(bpy)_3^{2+}$ molecule. An important reason for this is the relative shortness of the lifetime of the emissive ^{3}MLCT-excited state in the osmium complex: with ~50 ns it is more than an order of magnitude shorter than for $Ru(bpy)_3^{2+}$. Thus, electron transfer from or to ^{3}MLCT-excited $Os(bpy)_3^{2+}$ has to proceed with rate constants on the order of $10^7\ s^{-1}$ or greater in order for the photoredox reactions to be competitive with internal excited-state deactivation. This practically precludes electron transfer over very long (> 15 Å) distances. One of the relatively rare examples of a long-range electron transfer system with an osmium(II)-based photosensitizer is shown in Fig. 21 [79,80] comprised of a bis(4'-*p*-tolyl-2,2′:6′,2″-terpyridine) osmium(II) complex, $Os(ttpy)_2^{2+}$, with a covalently attached methylviologen molecule. This particular osmium(II) complex (without appended viologen) has a ^{3}MLCT lifetime of 240 ns in deoxygenated acetonitrile solution. With a methylviologen acceptor attached to it, this lifetime shortens to 0.72 ns, which is attributed to oxidative quenching of the ^{3}MLCT-excited state: the osmium(II) acts as an electron donor, the methylviologen as an acceptor. The center-to-center donor–acceptor distance is ~12 Å. Even in the absence of transient absorption data the interpretation of the excited-state quenching in terms of electron transfer is safe because triplet–triplet energy transfer is expected to be highly endergonic (ΔG_{EnT} = +1.3 eV), whereas electron transfer is exergonic (ΔG_{ET} = −0.55 eV). These in-depth physical studies were conducted by Amouyal, but the dyad from Fig. 21 was synthesized in the laboratories of Sauvage and Collin [80], who, in their initial paper, also provided the proof-of-concept for electron transfer in this osmium(II)–methylviologen dyad. A later collaboration between the Strasbourg group and Flamigni led to the conclusion that relaxation of the charge-separated state in the dyad from Fig. 21 must be faster than its formation [35]. In other words, a significant population of the charge-separated state cannot build up, and therefore attempts to detect the methylviologen radical by transient absorption spectroscopy are bound to fail.

Sauvage, Collin and coworkers also synthesized triads that are based on the dyad shown in Fig. 21; they contain phenothiazine (PTZ) and di-*p*-anisylamine (DPAA) donors that were attached covalently to the methyl group of the unsubstituted tolylterpyridine ligand in Fig. 21 [81]. The photophysics of these two triads were investigated by Barigelletti, De Cola, Flamigni, and Balzani. Unfortunately, for neither of the two systems a fully charge-separated state comprised of an oxidized PTZ or DPAA donor and a reduced methylviologen acceptor could be observed by means of transient absorption spectroscopy. In the case of the PTZ donor this has been attributed to the inefficiency of PTZ-to-osmium electron transfer due to weak electronic coupling (caused by a $-CH_2-$ spacer). In the DPAA triad, the fully charge-separated state is presumed to be too short-lived. This research has already been reviewed [11].

2.3.2. Conformational switching between long-range charge and energy transfer

In recent work, Lainé, Campagna, and coworkers investigated a series of osmium-based dyads as shown in Fig. 22 [82]. They are comprised of an osmium(II) bis(tolylterpyridine) photosensitizer, $Os(ttpy)_2^{2+}$, that bears a covalently attached triarylpyridino acceptor. Interesting photophysical properties, markedly different from those of the $Os(ttpy)_2^{2+}$ parent complex, arise when the triarylpyridino acceptor is substituted with an electron withdrawing nitro-group. In this case, photoinduced electron transfer from the metal center to the triarylpyridino moiety becomes thermodynamically possible; electrochemical studies indicate that the redox-active triarylpyridino orbital is very delocalized and probably extends over several rings. This pyridinium reduction is also expected to induce a planarization of the acceptor because of a quinoid-like electronic structure in the radical. Indeed, seemingly subtle conformational changes were found to play a major role in the dyads from Fig. 22: ultrafast transient absorption experiments reveal that upon osmium excitation, there are spectroscopic changes (occurring on a <10 ps timescale) that are consistent with a decrease of the torsion angle between the two aryl rings and the two terpyridine ligands to which they are directly attached to. In other words, each of the two tolylpyridine ligands planarizes upon photoexcitation. When considering the osmium(II) bis-terpyridine fragment as the donor, the central aryl as a bridge, and the pyridinium as an acceptor, this can be interpreted as enhanced donor–bridge electronic coupling in the excited state relative to the ground state. It turns out that for the long-range electron transfer properties of these osmium dyads yet another conformational effect is decisive, namely the torsion angle between the bridging aryl and the pyridinium governing bridge–acceptor electronic coupling. In a crystal structure of the dyad with a *m*-xylene bridge, this angle was found to be 74° which compares to 72° for the system with an unsubstituted phenyl-bridge. Thus, the methyl substituents do not appear to have a significant influence on the ground-state equilibrium bridge–acceptor torsion angle. However, they lock the tilted conformation and reduce the amplitude of thermal structure variation, thereby preventing any transient partial planarization of the bridge–acceptor entity. This is important as the comparison of the phenyl and *m*-xylyl bridged dyads from Fig. 22 with transient absorption experiments demonstrate: in the xylyl system the data is consistent with an osmium-to-pyridinium *electron* transfer, but for

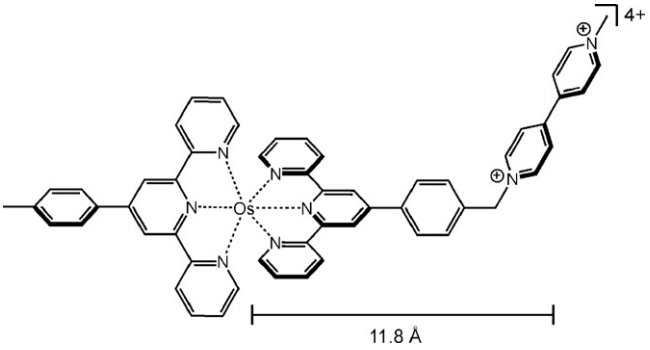

Fig. 21. Osmium(II) bis(4′-tolylterpyridine)–methylviologen dyad [79,80].

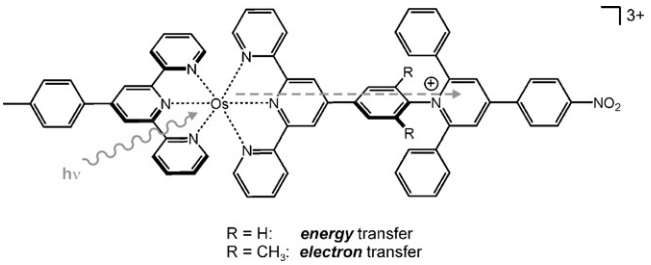

Fig. 22. Osmium(II)–pyridinium dyads that exhibit conformationally gated photoinduced processes [82,83].

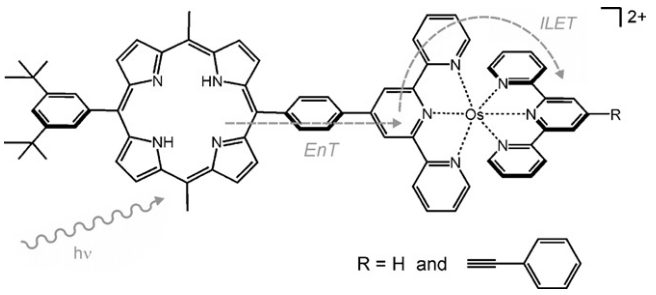

Fig. 23. A porphyrin–osmium system that is useful for the investigation of an interligand electron transfer (ILET) process. EnT denotes an energy transfer process [84].

the phenyl dyad it points to osmium-to-nitroarene (triplet–triplet) *energy* transfer. This is striking in view of the thermodynamics which are virtually identical for the two systems: electron transfer is weakly exergonic, energy transfer very weakly endergonic for both. The conformational effects mentioned above are invoked to explain the distinct photophysical properties: in the conformationally locked xylyl system, bridge–acceptor coupling stays weak at all times, but the phenyl system can adopt non-equilibrium conformations (bridge–acceptor torsion angles) that allow for transiently improved electronic coupling. This latter scenario is beneficial for triplet–triplet energy transfer occurring by an electron double exchange mechanism, since this process has a stronger dependence on electronic coupling than the transfer of a single electron. Thus, the energy transfer in the phenyl dyad is conformationally gated, and it kinetically outcompetes electron transfer. The sterically more demanding xylyl bridge impedes this conformational gating, the energy transfer is slowed down, and only the electron transfer stays competitive with other excited-state deactivation processes. The interpretation of these experimental results has been supported by a theoretical analysis that is based on density functional theory [83].

2.3.3. Interligand electron transfer

An interesting osmium(II)-based dyad, albeit not strictly a long-range electron transfer system has been reported recently by Harriman, Benniston, and coworkers [84]. This dyad, shown in Fig. 23, is comprised of an $Os(tpy)_2^{2+}$ complex that is attached, via a *p*-phenylene bridge, to a free-base porphyrin. Irradiation of this molecule with visible light primarily excites the porphyrin, which then transfers the excitation energy to the $Os(tpy)_2^{2+}$ unit, where singlet–triplet intersystem conversion occurs. The result is a ^{3}MLCT-excited osmium complex with the excited electron located selectively on the proximal tpy ligand. This excited state is deactivated by two competing processes: in the dyad with R = H, the dominant process is triplet–triplet (back) energy transfer to the porphyrin. In the dyad with R = phenylacetylene, the dominant process is an interligand electron transfer (ILET) from the proximal to the distal terpyridine ligand. This changeover in the main deactivation pathway upon substitution of the distal tpy ligand is a matter of increasing the driving-force for the ILET process. In the phenylacetylene substituted dyad it is exergonic by 0.04 eV, and occurs with a time constant of 10 ps. This was determined from a global fit to transient absorption data that show the kinetics of porphyrin singlet excited state disappearance, $Os(tpy)_2^{2+}$ ^{3}MLCT-excited state formation and decay, as well as porphyrin triplet excited-state formation. Thus, the observation of the ILET process is indirect. In the free $Ru(bpy)_3^{2+}$ and $Os(bpy)_3^{2+}$ complexes ILET occurs with time constants of 47 and 9 ps, respectively [85,86]. However, experimental measurements on these and other symmetrical complexes suffer from the fact that a statistical mixture of ^{3}MLCT states is produced upon photoexcitation. In the dyad from Fig. 23 this problem is overcome elegantly by covalent attachment of a porphyrin photosensitizer to one of the tpy ligands.

2.4. Iridium(III)

Polypyridine complexes of iridium(III) are isoelectronic to those of ruthenium(II). Yet, the photophysical and electrochemical properties of the two types of coordination compounds are quite distinct from one another. The energy of the lowest lying MLCT-excited state is substantially higher for the Ir(III) than for the Ru(II) complexes, reflecting the fact that a trivalent cation is more difficult to oxidize than a divalent cation. As a consequence, the lowest MLCT and LC excited states are energetically close to one another in iridium(III) polypyridines. Due to the strong ligand field that the 5d metal experiences in these complexes, the d-d excited states are at even higher energies, and a lowest energetic excited state of mixed LC and MLCT character results [87]. The spin multiplicity of this state is triplet, the energy gap to the ground state is large, and longer excited-state lifetimes than for ruthenium(II) polypyridine complexes often result. This is an advantage for photoredox studies since excited-state electron transfer reactions become more competitive with relaxation to the ground state. A second favorable feature of the iridium(III) polypyridines is that in their excited states they are more than 500 mV more oxidizing than most of the ruthenium(II) analogues. Thus, even when weak reductants are involved, iridium(III) polypyridine donor–acceptor systems exhibit efficient electron transfer. Despite these two favorable properties, iridium(III) polypyridines have received much less attention than the ruthenium(II) polypyridines. Among the key reasons for this are: (i) the ruthenium complexes are better light harvesters than the iridium complexes in that they absorb a much greater fraction of visible light; (ii) the ruthenium complexes are synthetically much more tractable than the iridium complexes; (iii) undesired energy transfer processes are more likely to interfere with desired electron transfer reactions in the iridium complexes: their emission occurs at relatively high energy and spectral overlaps with the absorption of other molecular components are more prone to occur in iridium-based donor–bridge–acceptor molecules than in ruthenium-based systems.

2.4.1. Iridium bis(terpyridine)–porphyrin systems

Building on their own prior work on donor–acceptor systems incorporating ruthenium(II) bis(terpyridine) cores, the research groups around Collin, Sauvage, and Flamigni have reported recently on several triads that contain the isostructural iridium(III) bis(terpyridine) unit [88]. In the triads from Fig. 24 this unit is substituted at the 4′-positions of the two tpy ligands: one tpy ligand bears a covalently attached free-base or zinc(II) porphyrin donor (H_2P or ZnP), the other a covalently attached gold(III) porphyrin acceptor (AuP). This substitution pattern allows the synthesis of linear systems in which the donor and acceptor lie in opposite directions, whereby the charge-separation distance is maximized. Thanks to the phenyl-bridges, the individual chromophores are only weakly coupled to one another, and a donor–acceptor distance of ~30 Å results. Excitation of the triad with M = H_2 at 592 nm leads to a free-base porphyrin luminescence that is strongly quenched with respect to a free-base porphyrin reference molecule that has no iridium complex nor gold(III) porphyrin attached to it. In addition, the singlet excited-state lifetime is reduced by more than two orders of magnitude. Transient absorption measurements on a dyad reference molecule comprised of only the free-base porphyrin and the iridium bis(tpy) complex reveal a rapid (~30 ps) formation of a free-base porphyrin radical cation, indicating that electron transfer from this porphyrin to the iridium(III) complex is very efficient. The same radical is also observed transiently in the

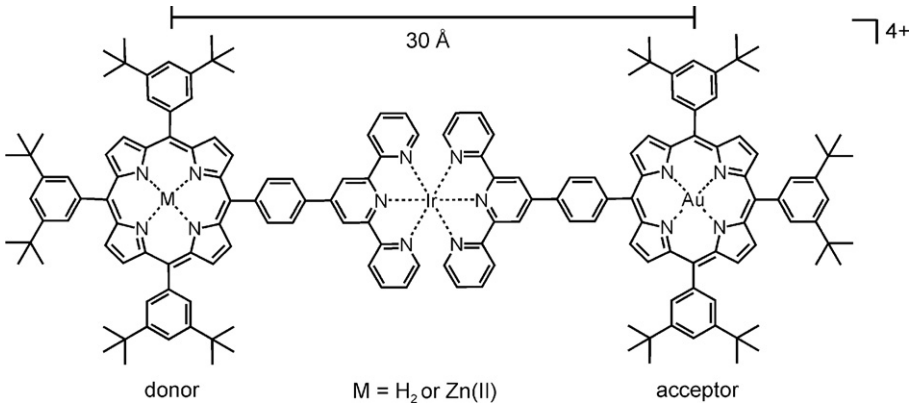

Fig. 24. Triads based on an iridium(III) bis(terpyridine) core acting as a photosensitizer for long-range electron transfer from a free-base (H_2P) or zinc(II) porphyrin (ZnP) donor to a gold(III) porphyrin (AuP) acceptor [88,89].

abovementioned free-base triad (M = H_2) from Fig. 24, but in this more sophisticated molecule the decay of the respective transient absorption signal is not only a factor of two faster than in the dyad reference molecule, but it also evolves over time into an absorption spectrum that is typical for the one-electron reduced gold(III) porphyrin. In other words, two sequential electron transfer as illustrated in the left part of Fig. 25 are observed: electron transfer from the photoexcited free-base porphyrin ($^{1*}H_2P$) to the iridium(III) core ("Ir") followed by electron transfer from the reduced iridium core ("Ir$^-$") to the gold(III) porphyrin (AuP). The lifetime of the H_2P^+–Ir–AuP$^-$ fully charge-separated state is 3 ns, and its main deactivation pathway is relaxation to an excited state that is best described as a free-base porphyrin-localized triplet excited state ($^{3*}H_2P$).

When the free-base porphyrin electron donor in Fig. 24 is replaced by a zinc(II) porphyrin, the energy of the fully charge-separated state is lowered by almost 0.3 eV, and the energy of the porphyrin-localized triplet state is raised by ~0.1 eV [89]. As a consequence, in the zinc(II) porphyrin system the ^{3}ZnP state is energetically above the fully charge-separated state, see the right part of Fig. 25. This leaves relaxation to the ground state as the only possible deactivation pathway for the fully charge-separated state. Consequently, the latter is more than two orders of magnitude longer lived (τ = 450 ns). In both triads the fully charge-separated state is attained with high quantum efficiency η: ~0.5 in the H_2P-triad and ~1.0 in the ZnP-triad.

2.4.2. *Iridium bis(terpyridine)-non-porphyrin systems*

In a synthetically very challenging study, the same researchers have investigated the triad shown in Fig. 26 in which a tertiary amine electron donor (triphenylamine, TPA) was linked to a naphthalene diimide (NDI) electron acceptor via the iridium(III) bis(terpyridine) motif ("Ir") [90]. As in the above study, a comparison with suitable dyads that served as reference molecules turned out to be indispensable to elucidate fully the more complicated photophysics of the triad [91]. This work revealed the occurrence of an efficient (η = 1.0) electron transfer process between the TPA unit and the Ir(tpy)$_2^{3+}$ core upon photoexcitation of the latter at 337 nm: within less than 20 ps the TPA is oxidized. This process is so exergonic ($-\Delta G_{ET}$ > 1 eV) that it even occurs in a frozen butyronitrile glass matrix at 77 K. Only once the iridium complex has been reduced by the TPA, it becomes a sufficiently potent donor for electron transfer to occur to the NDI acceptor. Thus, once the primary charge-separated state TPA$^+$–Ir$^-$ has been formed, two different things can happen: (i) the system can return to its ground state by back electron transfer (and it does so with a time constant of ~70 ps); (ii) a fully charge-separated state best described as TPA$^+$–Ir–NDI$^-$ can form (and this happens with a time constant of ~420 ps). It follows from these two time constants that the branching ratio is 6:1 in favor of the (undesired) charge-recombination process. Thus, only 1 in 7 photons absorbed leads to the formation of the fully charge-separated state in the triad from Fig. 26, whereas in the porphyrin systems from Fig. 24 it was 1 in 2 photons

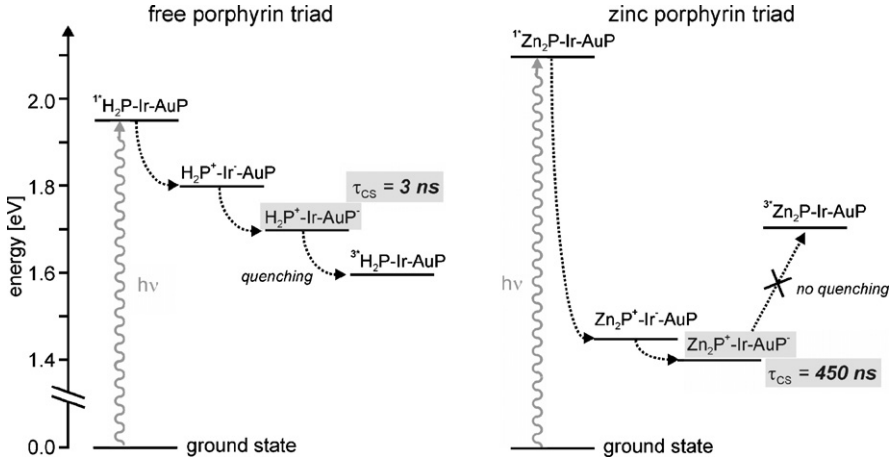

Fig. 25. Schematic representation of the photophysical processes occurring in the iridium(III) triads from Fig. 24. Here, "Ir" denotes the Ir(tpy)$_2^{3+}$ complex; "Ir$^-$" is its one-electron reduced form [88,89].

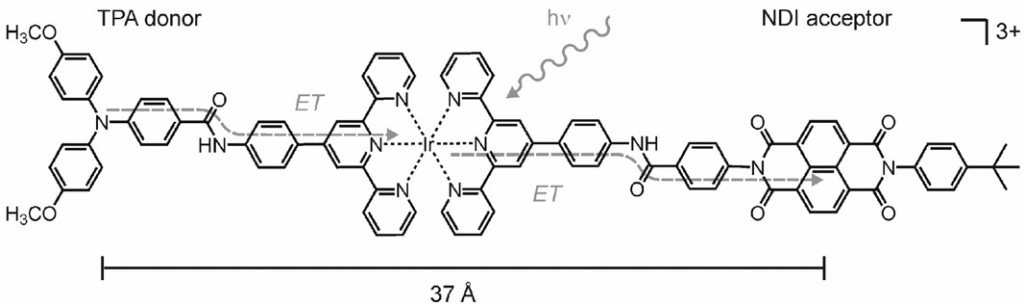

Fig. 26. An iridium(III)-based triad for photoinduced charge-separation over 37 Å [90,92].

(for the H_2P donor) and 1 in 1 photon (for the ZnP donor), respectively. It is with respect to the *lifetime* of the fully charge-separated state that the newer triad from Fig. 26 excels over the older systems from Fig. 24 and many other photoredox systems known to date. The TPA^+–Ir–NDI^- state decays with a time constant of 120 μs in deoxygenated acetonitrile solution as determined from transient absorption measurements that monitor both the disappearance of the TPA^+ radical cation at 475 nm and the NDI^- radical anion at 760 nm. The energy stored in this state amounts to 1.26 eV. This is a relatively large amount of energy that must be liberated upon return to the ground state. It is possible that this back electron transfer process is well in the Marcus inverted region which may explain the long lifetime of the fully charge-separated state. Remarkably, in aerated solution its lifetime is reduced by only 15%.

Due to its very long lifetime, a significant population of the TPA^+–Ir–NDI^- state may build up following photoexcitation of the triad in Fig. 26, particularly when high excitation densities are used. Indeed the associated transient absorption spectra as well as their decay profiles were found to be strongly dependent upon the excitation laser power [92]. At low powers one observes the two 120 μs-lived absorption bands due to TPA^+ and NDI^- radicals as described above. At high powers, an additional third band around 700–800 nm is observed. This has been assigned to an $Ir(tpy)_2{}^{3+}$ localized electronic transition: the TPA^+–Ir–NDI^- charge-separated state (with the iridium complex formally in its ground state) is promoted to a TPA^+–*Ir–NDI^- charge-separated state with the iridium core excited to a triplet excited state. In other words, one observes a sequence of charge-separation and excited-state absorption processes. The overall process must therefore involve the absorption of at least two photons, hence its strong laser power dependence. For sufficiently high powers the effect on the lifetime of the TPA^+–Ir–NDI^- fully charge-separated state becomes very spectacular: a shortening from 120 μs to 20 ns has been observed.

2.4.3. Cyclometalated iridium(III)

This class of compounds, although known since more than three decades [93], has received most attention only in recent years. The sudden increase of research activity in this area has to do with the relatively recent discovery that the electronic structure of cyclometalated iridium(III) complexes can be controlled deliberately through structure and ligand variations [94]. For instance, the emission color can be tuned throughout the entire visible range [95], making these compounds attractive for the implementation of organic light emitting diodes that include heavy metal triplet emitters. On the other hand, cyclometalated iridium(III) complexes have also become of interest for photocatalytic water splitting [96], bioanalytical applications [95], and oxygen sensing [97,98].

A recent study reports on an Ir(*p*-tolylpyridine)$_2$(2,2′-biimidazole)]$^+$ complex, Fig. 27, that forms hydrogen-bonded 1:1 adducts with carboxylate anions in apolar dichloromethane solution [99]. When the carboxylate is 3,5-dinitrobenzoate, the resulting supramolecular entity acts as a donor–acceptor dyad: upon photoexcitation the metal complex becomes a potent reductant, and this triggers an electron transfer through the hydrogen bonds to the dinitrobenzoate acceptor occurring over a distance of almost 10 Å. Spectroscopic evidence indicates that the electron transfer is accompanied by a significant redistribution of proton density within the salt bridge.

3. d^8 metal systems

3.1. Iridium(I) dimers

Pyrazolyl-bridged dinuclear iridium(I) complexes have long been known as particularly powerful photoreductants. For instance, the excited-state reduction potential of [Ir(μ-pz)(COD)]$_2$ (μ-pz = μ-pyrazolyl; COD = 1,5-cyclooctadiene) is −1.8 V vs. SCE in fluid acetonitrile solution [100]. Very large driving-forces (>1.5 eV) for photoinduced electron transfer reactions between this donor and 1,4-benzoquinone acceptors are the result. This makes investigations of phototriggered charge transfer in rigid media at cryogenic temperatures possible. Gray, Winkler, and coworkers have investigated long-range electron tunneling through glassy solvents at 77 K with this electron donor [21,101–103]. In 2-methyltetrahydrofuran and toluene glasses at liquid nitrogen temperature, the [Ir(μ-pz)(COD)]$_2$ complex emits red light with a lifetime of 3.2 μs. In the presence of randomly dispersed 2,6-dichloro-1,4-benzoquinone this emission is quenched significantly. The iridium excited-state depopulation becomes strongly non-exponential because of the wide distribution of donor–acceptor distances present in the sample (Fig. 28). Importantly, due to the rigidity of the glassy solvent matrix, these donor–acceptor distances are constant on the timescale of the electron transfer events. Thus, under the assumption that a statistical distribution of donors (present at μM concentration) and acceptors (at mM concentrations) is obtained, it is possible to extract distance decay parameters β for the phototriggered electron tunneling

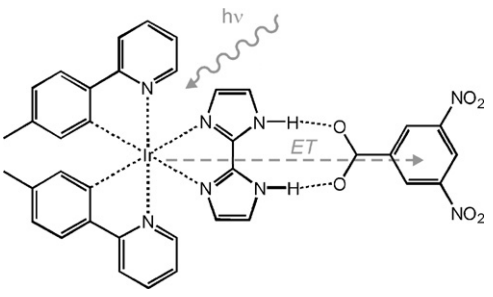

Fig. 27. Electron transfer across hydrogen-bonds in a donor–acceptor adduct [99].

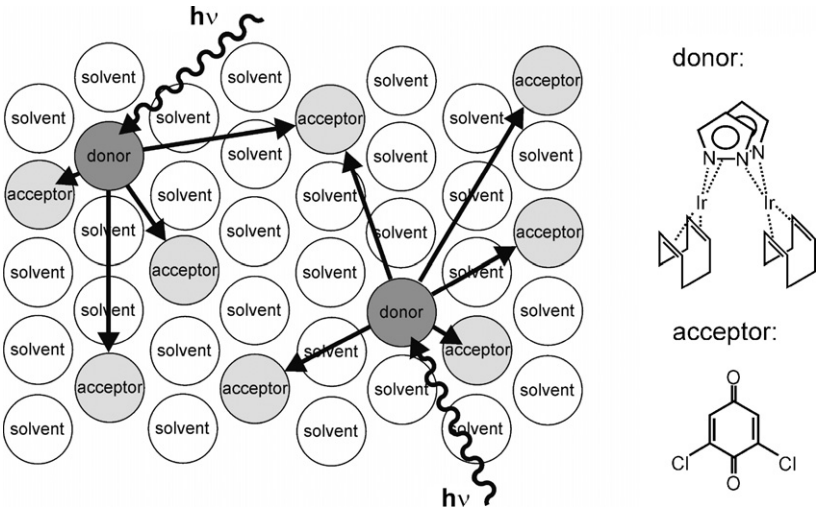

Fig. 28. Charge–neutral dinuclear iridium(I) donors and 2,6-dichloro-1,4-benzoquinone acceptors are randomly dispersed in frozen solvent glasses at 77 K. Selective photoexcitation of the donors leads to electron tunneling to acceptors at various distances, manifesting itself in strongly nonexponential luminescence lifetime quenching [102,103].

from the iridium complex to the benzoquinone. The β-values are 1.62 $Å^{-1}$ for 2-methyltetrahydrofuran and 1.23 $Å^{-1}$ for toluene, i.e., toluene is mediating the long-range electron tunneling significantly better than 2-methyltetrahydrofuran. To illustrate this point it may be noted that a 20 Å tunneling step proceeds ~3 orders of magnitude faster through toluene than through 2-methyltetrahydrofuran [102,103]. This observation suggests that so-called tunneling energy effects play a decisive role in determining long-range electronic coupling; aromatic molecules (toluene) have lower lying energy levels than saturated organic bridges (2-methyltetrahydrofuran), and this leads to enhanced electronic coupling between donor and acceptor [104]. Importantly, this work also allows estimation of the (in)efficiency of electron tunneling across van der Waals gaps, namely by comparison with the previously determined distance decay parameters for covalent alkane bridges and rigid rod-like oligo-*p*-phenylene spacers. Electron tunneling through a 2 Å van der Waals gap is ~50 times slower than tunneling the same distance through covalently bonded bridge. This observation has important implications for biological long-range electron transfer: the medium between redox centers in proteins is a heterogeneous array of covalent, hydrogen-bond, and van der Waals contacts between atoms of the polypeptide matrix. The protein secondary and tertiary structure must ensure that there exist tunneling pathways with many covalent and hydrogen bonds but with few van der Waals gaps such that electron tunneling can occur efficiently over long distances.

3.2. Platinum(II) acetylides

3.2.1. The Rochester work

Platinum polyimine acetylide complexes have been identified rather recently as suitable systems for long-range electron transfer investigations. Eisenberg and coworkers established that the long-lived emissive excited states of Pt diimine bis(acetylide) complexes are actually ^{3}MLCT states that can undergo photoredox chemistry [105]. Indeed the nature of this excited state appears to be similar to the charge transfer states of the d^6 diimine complexes discussed above. This has prompted investigation of covalent donor–acceptor dyads and triads that are based on this or closely related chromophores [106–108]. Cases in point are the systems shown in Fig. 29 which have phenothiazine donors appended to the platinum(II) complexes [106]. Reference complexes without these tertiary amines have ^{3}MLCT lifetimes of the order of 500 ns depending on the exact bpy-substitution pattern and the solvent. When the dyad from Fig. 29 with R = *t.*-Bu and R′ = H is investigated under relatively polar solvent conditions (acetonitrile, dichloromethane) the ^{3}MLCT-excited state decays within less than 1 ns. Electrochemical and UV–vis studies have shown that electron transfer from the phenothiazine-nitrogen to the photoexcited platinum complex are exergonic. Indeed, picosecond time-resolved transient absorption experiments reveal the formation of a phenothiazine radical cation. In the dyad with R = *t.*-Bu and R′ = CF_3 this species forms with a time constant of 0.56 ns which explains the ^{3}MLCT luminescence lifetime quenching mentioned above. Through chemical variation of the R-substituents at the bpy ligand and the R′-substituent at the phenothiazine it is possible to tune the driving-force for this photoinduced charge transfer. Replacement of R = *t.*-Bu with R = CO_2Et lowers the energy of the ^{3}MLCT state by ~3000 cm^{-1}, and the excited platinum complex becomes significantly more oxidizing. On the other hand, by substituting the phenothiazine with the electron-withdrawing trifluoromethyl group, this donor becomes less potent. Experimentally, charge transfer rates were found to increase along the series of three dyads with (i) R = *t.*-Bu, R′ = CF_3; (ii)

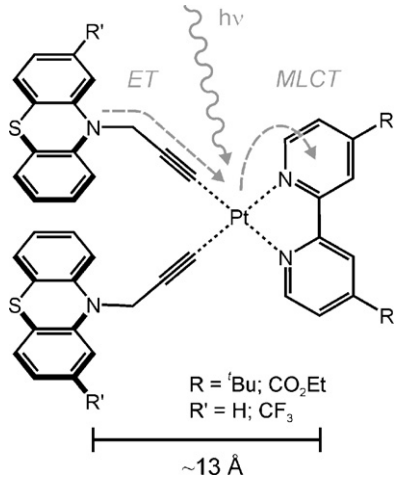

Fig. 29. Platinum(II) complexes with covalently attached phenothiazine donors [106].

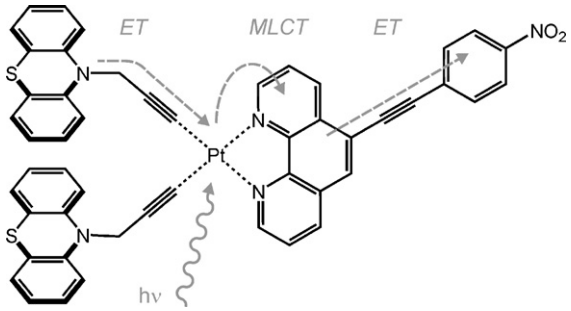

Fig. 30. Triad comprised of two phenothiazine donors, a platinum bis(acetylide) photosensitizer complex, and a nitrobenzene acceptor [107,108].

R = *t*.-Bu, R′ = H; (iii) R = CO_2Et, R′ = H. Thus, the charge-separation rates increase with increasing driving-force $-\Delta G_{CS}$, consistent with electron transfer in the Marcus normal region. This is no surprise because in absolute terms $-\Delta G_{CS}$ is small (0.1–0.2 eV) for all systems considered. This also explains the strong solvent dependence of the photoredox chemistry of these dyads, in particular why electron transfer does not occur in the apolar toluene solvent: decreasing solvent polarity destabilizes the HOMO of the Pt complex (the MLCT absorption maximum red-shifts by ~2500 cm^{-1} when going from acetonitrile to toluene) which lowers the driving-force for electron transfer from the phenothiazine to this Pt orbital (which is singly occupied in the MLCT-excited state). An interesting observation is that in polar solvents the quantum yield for formation of the charge-separated state is independent on the ^{3}MLCT-excited state lifetime. Charge-recombination is much slower than charge-separation in all three dyads; time constants range from 1.4 to 6 ns. It is likely that an inverted driving-force effect is at work since the recombination processes are highly exergonic (−2.0 eV).

Fig. 30 shows the first triad in which the chromophore is a Pt diimine complex [107]. In addition to the phenothiazine donors already present in the dyads above, this molecule has a 1,10-phenanthroline ligand which bears a covalently attached nitrophenyl acceptor. The luminescence of the d^8 metal chromophore in this system is quenched completely, and transient absorption spectroscopy revealed the formation of both a phenothiazine radical cation (with a characteristic absorption at 525 nm) and a nitrobenzene radical anion (with an absorption at 455 nm). At the same time the nitrophenyl ground-state absorption at 360 nm was bleached. These results are consistent with the formation of a fully charge-separated state in which an electron has formally traveled from the phenothiazine to the nitrobenzene. This state transiently stores 1.67 eV, and its lifetime is 70 ns.

Subsequent research focused on the platinum(II) terpyridyl arylacetylide chromophore which allows construction of linear donor–chromophore–acceptor triads such as the molecule shown in Fig. 31 [108]. An important advantage of this chromophore with respect to platinum diimine bis(arylacetylide) systems is the fact that the resulting molecules are positively charged, which imparts solubility on these systems. In the triad of Fig. 31 the edge-to-edge separation between the trimethoxybenzene donor and the pyridinium acceptor is ~28 Å as determined from an X-ray crystal structure. As anticipated, the emission of the platinum chromophore in this triad is quenched completely and from a comparison with a reference dyad (comprised of the trimethoxybenzene donor and the platinum chromophore but lacking the pyridinium), this excited-state quenching could be attributed to trimethoxybenzene-to-platinum electron transfer. However, transient absorption experiments on the triad from Fig. 31 as well as studies on an appropriate chromophore–pyridinium dyad show that the pyridinium acceptor is not involved in charge transfer in these systems. In order to obtain a fully charge-separated state, the terminal acceptor had to be changed, and this was accomplished in the triads shown in Fig. 32 [108]. The ~700 ns lifetime of the platinum tolylterpyridine phenylacetylide chromophore in this triad is quenched to <30 ns. This molecule has a phenothiazine donor and a nitrostilbene unit as a terminal acceptor. Transient absorption spectroscopy shows that by contrast to the pyridinium in the triad from Fig. 31, the nitrostilbene acceptor quenches the platinum excited state oxidatively. The spectroscopic evidence for this is a transient absorption signal around ≥450 nm, assigned to the nitrostilbene radical anion, and the phenothiazine radical cation (PTZ^+) signature is observed simultaneously. Thus, a fully charge-separated state (PTZ^+–Pt–nitrostilbene$^-$ or D^+–C–A^-) is formed in this system. An interesting aspect is how the population of this state builds up. Initial photoexcitation promotes the platinum complex to its ^{3}MLCT state (D–C*–A, Fig. 33).

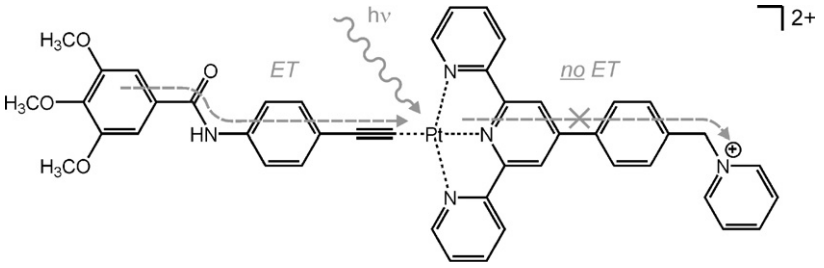

Fig. 31. The Pt(II) terpyridyl unit allows for the synthesis of nearly linear donor–chromophore–acceptor systems. The pyridinium acceptor is inactive in this molecule [108].

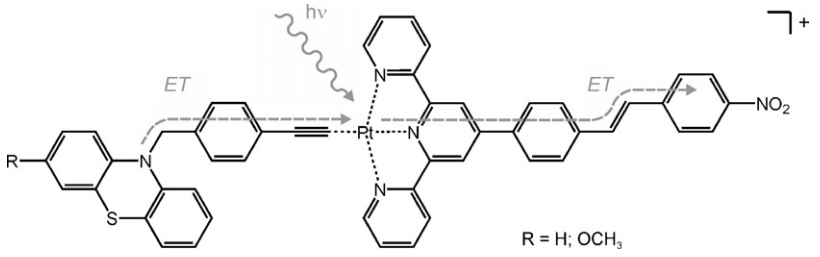

Fig. 32. Triad for long-range electron transfer from a phenothiazine to a nitrostilbene; the overall process is triggered by Pt excitation [108].

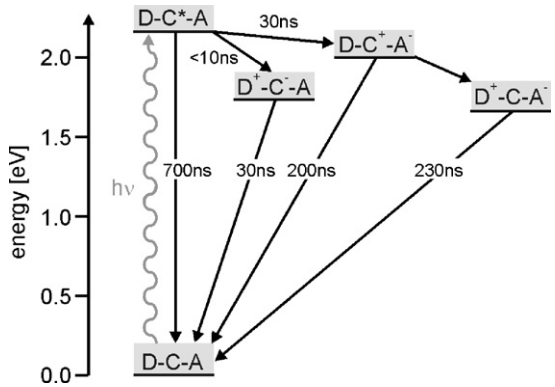

Fig. 33. Schematic summary of the photoredox processes occurring in the triad from Fig. 32 [108].

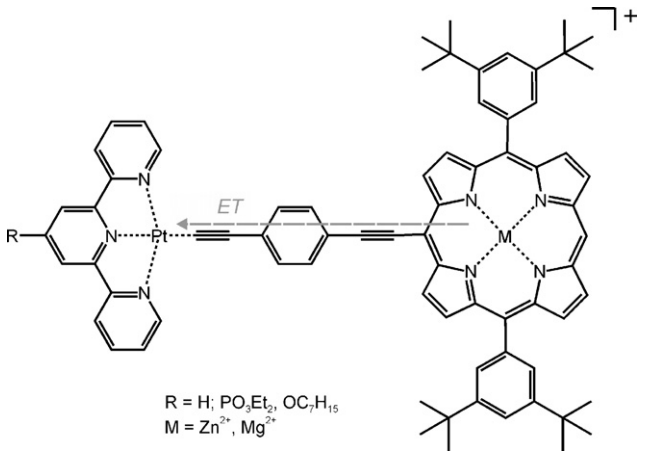

Fig. 34. Porphyrin–platinum dyads for driving-force investigations of long-range electron transfer [109].

Detailed mechanistic studies reveal that reductive quenching of this state is at least three times more efficient than oxidative quenching. In other words, there is a branching ratio that is in favor of a donor$^+$–chromophore$^-$–acceptor (D^+–C^-–A) rather than a donor–chromophore$^+$–acceptor$^-$ (D–C^+–A^-) intermediate state. This is attributed to the fact that the formation of the former is energetically more favorable by ~0.3 eV. The inherent lifetimes of these two charge-separated states in appropriate D–C and C–A dyads differ by almost an order of magnitude: the D^+–C^- state decays to the ground state with τ = 30 ns, whereas the C^+–A^- state has a lifetime of 200 ns. Logically, in the triad secondary electron transfer that establishes the fully charge-separated state (D^+–C–A^-) is much more competitive with relaxation to the ground state in the longer-lived D–C^+–A^- state. As a consequence, although reductive quenching predominates for the triad upon excitation, forward electron transfer to generate the fully charge-separated state does not happen primarily by this route. Instead, slower oxidative quenching leads to an intermediate which then rapidly advances to the fully charge-separated state rather than undergoing back reaction to the ground state. This unusual quenching pattern has important implications for the efficiency of formation of the fully charge-separated state: a rough estimate is that only 25–30% of the excited triad with R = H (Fig. 32) leads to the fully charge-separated species. The lifetime of this state is three times longer than that of the triad from Fig. 30. This may be due to the greater donor–acceptor separation in the terpyridyl-triad as well as better solvation resulting from the cationic charge on this complex.

3.2.2. A platinum(II) acetylide–porphyrin dyad

Odobel, Hammarström, and coworkers have also used the platinum(II) terpyridyl acetylide chromophore for electron transfer investigations [109]. In the dyads shown in Fig. 34, excitation of the porphyrin unit induces a very rapid (2–20 ps) electron transfer to the covalently attached platinum complex. Through variation of the terpyridine R-substituent as well as through changing the metal that is complexed inside the porphyrin, it was possible to vary the driving-force for the photoinduced electron transfer. The lowest driving-force (ΔG_{ET} = −0.26 eV) resulted for the dyad with R = OC_7H_{15} and M = Zn^{2+}. Replacement of the *n*-heptoxy by a diethylphosphonate group (R = PO_3Et_2) renders the platinum complex significantly more oxidizing, and when Zn^{2+} is replaced by Mg^{2+}, the porphyrin becomes a slightly better donor. Thus, the dyad with R = PO_3Et_2 and M = Mg^{2+} has the highest driving-force for photoinduced electron transfer (ΔG_{ET} = −0.66 eV). The rate constants k_{ET} for phototriggered porphyrin → platinum electron transfer vary from 5×10^{10} s^{-1} (for ΔG_{ET} = −0.26 eV) to 5×10^{11} s^{-1} (for ΔG_{ET} = −0.66 eV), i.e., they fall into the Marcus normal region. The six data points for the six investigated dyads can be fit well to a parabolic Marcus curve with λ = 0.65 eV, which is a reasonable value for a total reorganization energy for such systems. Unfortunately charge-recombination turned out to be even faster than charge-separation in all six systems; transient absorption experiments show that a significant population of the charge-separated state never builds up. An additional point is noteworthy: both optical absorption and electrochemical studies point to a significant electronic interaction between the porphyrin and the platinum complex. The porphyrin absorptions are slightly red-shifted (~5 nm) in the dyads, and the porphyrin reduction potential is susceptible to the chemical nature of the R-substituent on the platinum terpyridine complex. This indicates that the dyads in Fig. 34 are not weakly coupled donor–bridge–acceptor molecules, unlike most other systems considered in this review. It is possible that the donor and acceptor states are significantly delocalized over the bridge as has been previously observed for a series of phenylethynyl-bridged zinc(II) porphyrin–diimide dyads [110]. Distance dependence studies of electron transfer in Pt–phenylethynyl–porphyrin systems will be required to address this issue.

4. Summary

Complexes of d^6 and d^8 metal ions are of great interest for phototriggered long-range electron transfer studies since many of them have long-lived excited states from which charge transfer to distant redox partners is competitive with internal excited-state deactivation processes. Ruthenium(II) polypyridines continue to draw most attention. Isoelectronic complexes of iridium(III) have been identified as interesting alternatives, but their syntheses are much less straightforward. Osmium(II) polypyridines keep playing a subordinate role. As redox partners for long-range electron transfer initiating from the ^{3}MLCT-excited state of ruthenium(II) complexes they are well suited, but their own ^{3}MLCT lifetimes are too short for efficient long-range photoredox chemistry. Rhenium(I) tricarbonyl diimines continue to get limited attention as well, but their CO vibrations are now being recognized as useful spectroscopic observables for long-range electron transfer investigations by transient infrared absorption techniques. A significant novelty is the use of platinum(II) acetylide complexes as photosensitizers for charge transfer over long distances. Unfortunately they are less stable towards oxidative excited-state quenching than $Ru(bpy)_3^{2+}$-type complexes, and they appear to be significantly less soluble in common organic solvents. Despite these drawbacks, plat-

inum(II) acetylides are likely to get even increasing attention in the near future.

The construction of artificial systems with long-lived charge-separated states has remained a central issue in the field of long-range electron transfer. A commonly adopted strategy is to explore new donor/acceptor combinations that place the undesired thermal charge-recombination reactions into the Marcus inverted region whereby better discrimination between charge-separation and -recombination rates is sometimes obtained. Less, but clearly increasing effort has been devoted to the exploration of the role played by the bridge-mediated electronic donor–acceptor coupling. Evidence is building up that in some systems the electronic coupling may be significantly different for photoinduced forward and thermal backward electron transfer, and this may be a chance to further stabilize charge-separated states. There is also an increasing interest in long-range electron transfer reactions that are mediated by noncovalent contacts such as hydrogen bonds and van der Waals gaps.

Naturally, the investigation of these phenomena is not limited to d^6 and d^8 metal-based systems. The field of long-range electron transfer in artificial systems has seen much progress on porphyrin-based donor–bridge–acceptor molecules in recent years. Key activities include the construction of artificial antenna-reaction center molecules [51,53], the investigation of many novel porphyrin–fullerene systems some of which exhibit charge-separation over very long distances (> 40 Å) with extremely slow recombination rates [111–116], the in-depth study of bridging medium effects on long-range electron transfer with the help of porphyrin donors and acceptors [117–121], or even the use of porphyrin wires that themselves mediate charge transfer over long distances [122,123].

The actual exploitation of the light energy stored in the long-lived charge-separated states generated in artificial systems remains a significant challenge [124].

Acknowledgments

Financial support from the Swiss National Science Foundation is gratefully acknowledged. Two anonymous referees are thanked for their useful comments.

References

[1] M. Bixon, J. Jortner, M.E. Michel-Beyerle, Biochim. Biophys. Acta 1056 (1991) 301.
[2] P. Jordan, P. Fromme, H.T. Witt, O. Klukas, W. Saenger, N. Krauss, Nature 411 (2001) 909.
[3] B.E. Ramirez, B.G. Malmström, J.R. Winkler, H.B. Gray, Proc. Natl. Acad. Sci. USA 92 (1995) 11949.
[4] B.E. Bowler, A.L. Raphael, H.B. Gray, Progr. Inorg. Chem 38 (1990) 259.
[5] B. Giese, Acc. Chem. Res 33 (2000) 631.
[6] D.N. Beratan, J.N. Betts, J.N. Onuchic, Science 252 (1991) 1285.
[7] D. Gust, T.A. Moore, A.L. Moore, Acc. Chem. Res. 26 (1993) 198.
[8] F.D. Lewis, R.L. Letsinger, M.R. Wasielewski, Acc. Chem. Res. 34 (2001) 159.
[9] N.S. Hush, Coord. Chem. Rev. 64 (1985) 135.
[10] G.L. Closs, J.R. Miller, Science 240 (1988) 440.
[11] J.-P. Sauvage, J.-P. Collin, J.-C. Chambron, S. Guillerez, C. Coudret, V. Balzani, F. Barigelletti, L. De Cola, L. Flamigni, Chem. Rev. 94 (1994) 993.
[12] D.M. Guldi, Chem. Soc. Rev. 31 (2002) 22.
[13] G. McLendon, T. Guarr, M. McGuire, K. Simolo, S. Strauch, K. Taylor, Coord. Chem. Rev 64 (1985) 113.
[14] K.S. Schanze, D.B. MacQueen, T.A. Perkins, L.A. Cabana, Coord. Chem. Rev. 122 (1993) 63.
[15] G. McLendon, R. Hake, Chem. Rev. 92 (1992) 481.
[16] A. Hagfeldt, M. Grätzel, Acc. Chem. Res. 33 (2000) 269.
[17] H.B. Gray, J.R. Winkler, Ann. Rev. Biochem. 65 (1996) 537.
[18] M.R. Wasielewski, Chem. Rev. 92 (1992) 435.
[19] D. Gust, T.A. Moore, A.L. Moore, Acc. Chem. Res. 34 (2001) 40.
[20] V. Balzani, Electron Transfer in Chemistry, in: Biological and Artificial Supramolecular Systems, vol. 3, VCH Wiley, Weinheim, 2001.
[21] H.B. Gray, J.R. Winkler, Proc. Natl. Acad. Sci. USA 102 (2005) 3534.
[22] J. Stubbe, D.G. Nocera, C.S. Yee, M.C.Y. Chang, Chem. Rev. 103 (2003) 2167.
[23] S.S. Isied, M.Y. Ogawa, J.F. Wishart, Chem. Rev. 92 (1992) 381.
[24] M.N. Paddon-Row, Acc. Chem. Res. 27 (1994) 18.
[25] S.E. Peterson-Kennedy, J.L. McGourty, P.S. Ho, C.J. Sutoris, N. Liang, H. Zemel, N.V. Blough, E. Margoliash, B.M. Hoffman, Coord. Chem. Rev. 64 (1985) 125.
[26] L. De Cola, P. Belser, Coord. Chem. Rev. 177 (1998) 301.
[27] J.-P. Collin, A. Harriman, V. Heitz, F. Odobel, J.-P. Sauvage, Coord. Chem. Rev. 148 (1996) 63.
[28] L. Flamigni, F. Barigelletti, N. Armaroli, J.-P. Collin, I.M. Dixon, J.-P. Sauvage, J.A.G. Williams, Coord. Chem. Rev. 192 (1999) 671.
[29] I. Willner, E. Kaganer, E. Joselevich, H. Dürr, E. David, M.J. Günter, M.R. Johnston, Coord. Chem. Rev. 171 (1998) 261.
[30] M. Furue, K. Maruyama, Y. Kanematsu, T. Kushida, M. Kamachi, Coord. Chem. Rev. 132 (1994) 201.
[31] V. Balzani, A. Juris, Coord. Chem. Rev. 211 (2001) 97.
[32] M.H.V. Huynh, D.M. Dattelbaum, T.J. Meyer, Coord. Chem. Rev. 249 (2005) 457.
[33] J.R. Winkler, H.B. Gray, Chem. Rev. 92 (1992) 369.
[34] H. Dürr, S. Bossmann, Acc. Chem. Res. 34 (2001) 905.
[35] E. Baranoff, J.-P. Collin, L. Flamigni, J.-P. Sauvage, Chem. Soc. Rev. 33 (2004) 147.
[36] H.B. Gray, J.R. Winkler, D. Wiedenfeld, Coord. Chem. Rev. 200 (2000) 875.
[37] M. Hissler, J.E. McGarrah, W.B. Connick, D.K. Geiger, S.D. Cummings, R. Eisenberg, Coord. Chem. Rev. 208 (2000) 115.
[38] K.V. Mikkelsen, M.A. Ratner, Chem. Rev. 87 (1987) 113.
[39] P.F. Barbara, T.J. Meyer, M.A. Ratner, J. Phys. Chem. 100 (1996) 13148.
[40] G. Steinberg-Yfrach, P.A. Liddell, S.C. Hung, A.L. Moore, D. Gust, T.A. Moore, Nature 385 (1997) 239.
[41] V. Balzani, M. Venturi, A. Credi, Molecular Devices and Machines, VCH-Wiley, Weinheim, 2003.
[42] K.E. Berg, A. Tran, M.K. Raymond, M. Abrahamsson, J. Wolny, S. Redon, M. Andersson, L.C. Sun, S. Styring, L. Hammarström, H. Toftlund, B. Åkermark, Eur. J. Inorg. Chem. (2001) 1019.
[43] M.L.A. Abrahamsson, H.B. Baudin, A. Tran, C. Philouze, K.E. Berg, M.K. Raymond-Johansson, L.C. Sun, B. Åkermark, S. Styring, L. Hammarström, Inorg. Chem. 41 (2002) 1534.
[44] O. Johansson, M. Borgström, R. Lomoth, M. Palmblad, J. Bergquist, L. Hammarström, L.C. Sun, B. Åkermark, Inorg. Chem. 42 (2003) 2908.
[45] M. Borgström, N. Shaikh, O. Johansson, M.F. Anderlund, S. Styring, B. Åkermark, A. Magnuson, L. Hammarström, J. Am. Chem. Soc. 127 (2005) 17504.
[46] O. Johansson, H. Wolpher, M. Borgström, L. Hammarström, J. Bergquist, L.C. Sun, B. Åkermark, Chem. Commun. (2004) 194.
[47] Y.H. Xu, G. Eilers, M. Borgström, J.X. Pan, M. Abrahamsson, A. Magnuson, R. Lomoth, J. Bergquist, T. Polívka, L.C. Sun, V. Sundström, S. Styring, L. Hammarström, B. Åkermark, Chem. Eur. J. 11 (2005) 7305.
[48] S.W. Gersten, G.J. Samuels, T.J. Meyer, J. Am. Chem. Soc. 104 (1982) 4029.
[49] M. Borgström, O. Johansson, R. Lomoth, H.B. Baudin, S. Wallin, L.C. Sun, B. Åkermark, L. Hammarström, Inorg. Chem. 42 (2003) 5173.
[50] M. Borgström, S. Ott, R. Lomoth, J. Bergquist, L. Hammarström, O. Johansson, Inorg. Chem. 45 (2006) 4820.
[51] G. Kodis, P.A. Liddell, L. de la Garza, P.C. Clausen, J.S. Lindsey, A.L. Moore, T.A. Moore, D. Gust, J. Phys. Chem. A 106 (2002) 2036.
[52] D. Kuciauskas, P.A. Liddell, S. Lin, T.E. Johnson, S.J. Weghorn, J.S. Lindsey, A.L. Moore, T.A. Moore, D. Gust, J. Am. Chem. Soc. 121 (1999) 8604.
[53] R.F. Kelley, M.J. Tauber, M.R. Wasielewski, Angew. Chem. Int. Ed. 45 (2006) 7979.
[54] S. Campagna, S. Serroni, F. Puntoriero, F. Loiseau, L. De Cola, C.L. Kleverlaan, J. Becher, A.P. Sorensen, P. Hascoat, N. Thorup, Chem. Eur. J. 8 (2002) 4461.
[55] C. Goze, C. Leiggener, S.X. Liu, L. Sanguinet, E. Levillain, A. Hauser, S. Decurtins, Chem. Phys. Chem. 8 (2007) 1504.
[56] C. Leiggener, N. Dupont, S.X. Liu, C. Goze, S. Decurtins, E. Breitler, A. Hauser, Chimia 61 (2007) 621.
[57] S.A. Serron, W.S. Aldridge, C.N. Fleming, R.M. Danell, M.H. Baik, M. Sykora, D.M. Dattelbaum, T.J. Meyer, J. Am. Chem. Soc. 126 (2004) 14506.
[58] R.A. Malak, Z.N. Gao, J.F. Wishart, S.S. Isied, J. Am. Chem. Soc. 126 (2004) 13888.
[59] E. Galoppini, W.Z. Guo, W. Zhang, P.G. Hoertz, P. Qu, G.J. Meyer, J. Am. Chem. Soc. 124 (2002) 7801.
[60] M. Kercher, B. König, H. Zieg, L. De Cola, J. Am. Chem. Soc. 124 (2002) 11541.
[61] H.F.M. Nelissen, M. Kercher, L. De Cola, M.C. Feiters, R.J.M. Nolte, Chem. Eur. J. 8 (2002) 5407.
[62] J.M. Haider, M. Chavarot, S. Weidner, I. Sadler, R.M. Williams, L. De Cola, Z. Pikramenou, Inorg. Chem. 40 (2001) 3912.
[63] S. Weidner, Z. Pikramenou, Chem. Commun. (1998) 1473.
[64] J.M. Haider, Z. Pikramenou, Chem. Soc. Rev. 34 (2005) 120.
[65] J.-P. Launay, Chem. Soc. Rev. 30 (2001) 386.
[66] P.J. Mosher, G.P.A. Yap, R.J. Crutchley, Inorg. Chem. 40 (2001) 1189.
[67] A.C. Benniston, V. Grosshenny, A. Harriman, R. Ziessel, Dalton Trans. (2004) 1227.
[68] A. Gabrielsson, F. Hartl, J.R.L. Smith, R.N. Perutz, Chem. Commun. (2002) 950.
[69] A. Gabrielsson, F. Hartl, H. Zhang, J.R.L. Smith, M. Towrie, A. Vlček, R.N. Perutz, J. Am. Chem. Soc. 128 (2006) 4253.
[70] R. Lopez, A.M. Leiva, F. Zuloaga, B. Loeb, E. Norambuena, K.M. Omberg, J.R. Schoonover, D. Striplin, M. Devenney, T.J. Meyer, Inorg. Chem. 38 (1999) 2924.
[71] J.D. Lewis, L. Bussotti, P. Foggi, R.N. Perutz, J.N. Moore, J. Phys. Chem. A 106 (2002) 12202.

[72] A. Dirksen, C.J. Kleverlaan, J.N.H. Reek, L. De Cola, J. Phys. Chem. A 109 (2005) 5248.
[73] A. McNally, R.J. Forster, N.R. Russell, T.E. Keyes, Dalton Trans. (2006) 1729.
[74] D. Hanss, O.S. Wenger, Inorg. Chem 47 (2008) 9081.
[75] E.A. Weiss, M.J. Ahrens, L.E. Sinks, A.V. Gusev, M.A. Ratner, M.R. Wasielewski, J. Am. Chem. Soc. 126 (2004) 5577.
[76] Z.E.X. Dance, M.J. Ahrens, A.M. Vega, A.B. Ricks, D.W. McCamant, M.A. Ratner, M.R. Wasielewski, J. Am. Chem. Soc. 130 (2008) 830.
[77] A. Helms, D. Heiler, G. McLendon, J. Am. Chem. Soc. 114 (1992) 6227.
[78] M.T. Indelli, C. Chiorboli, L. Flamigni, L. De Cola, F. Scandola, Inorg. Chem. 46 (2007) 5630.
[79] E. Amouyal, M. Mouallem-Bahout, J. Chem. Soc. Dalton Trans. (1992) 509.
[80] J.-P. Collin, S. Guillerez, J.-P. Sauvage, J. Chem. Soc., Chem. Commun. (1989) 776.
[81] J.-P. Collin, S. Guillerez, J.-P. Sauvage, F. Barigelletti, L. De Cola, L. Flamigni, V. Balzani, Inorg. Chem 31 (1992) 4112.
[82] P.P. Lainé, F. Bedioui, F. Loiseau, C. Chiorboli, S. Campagna, J. Am. Chem. Soc. 128 (2006) 7510.
[83] P.P. Lainé, F. Loiseau, S. Campagna, I. Ciofini, C. Adamo, Inorg. Chem. 45 (2006) 5538.
[84] A.C. Benniston, A. Harriman, C. Pariani, C.A. Sams, J. Phys. Chem. A 111 (2007) 8918.
[85] A.T. Yeh, C.V. Shank, J.K. McCusker, Science 289 (2000) 935.
[86] G.B. Shaw, C.L. Brown, J.M. Papanikolas, J. Phys. Chem. A 106 (2002) 1483.
[87] C.M. Flynn, J.N. Demas, J. Am. Chem. Soc. 96 (1974) 1959.
[88] I.M. Dixon, J.-P. Collin, J.-P. Sauvage, F. Barigelletti, L. Flamigni, Angew. Chem. Int. Ed. 39 (2000) 1292.
[89] L. Flamigni, I.M. Dixon, J.-P. Collin, J.-P. Sauvage, Chem. Commun. (2000) 2479.
[90] L. Flamigni, E. Baranoff, J.-P. Collin, J.-P. Sauvage, Chem. Eur. J. 12 (2006) 6592.
[91] E. Baranoff, I.M. Dixon, J.-P. Collin, J.-P. Sauvage, B. Ventura, L. Flamigni, Inorg. Chem. 43 (2004) 3057.
[92] L. Flamigni, E. Baranoff, J.-P. Collin, J.-P. Sauvage, B. Ventura, ChemPhysChem. 8 (2007) 1943.
[93] M. Nonoyama, Bull. Chem. Soc. Jpn. 47 (1974) 767.
[94] S. Lamansky, P. Djurovich, D. Murphy, F. Abdel-Razzaq, H.E. Lee, C. Adachi, P.E. Burrows, S.R. Forrest, M.E. Thompson, J. Am. Chem. Soc. 123 (2001) 4304.
[95] M.S. Lowry, S. Bernhard, Chem. Eur. J. 12 (2006) 7970.
[96] M.S. Lowry, J.I. Goldsmith, J.D. Slinker, R. Rohl, R.A. Pascal, G.G. Malliaras, S. Bernhard, Chem. Mater. 17 (2005) 5712.
[97] F. Lafolet, S. Welter, Z. Popovic, L. De Cola, J. Mater. Chem. 15 (2005) 2820.
[98] V.L. Whittle, J.A.G. Williams, Inorg. Chem. 47 (2008) 6596.
[99] J.C. Freys, G. Bernardinelli, O.S. Wenger, Chem. Commun. (2008) 4267.
[100] J.L. Marshall, S.R. Stobart, H.B. Gray, J. Am. Chem. Soc. 106 (1984) 3027.
[101] A. Ponce, H.B. Gray, J.R. Winkler, J. Am. Chem. Soc. 122 (2000) 8187.
[102] O.S. Wenger, B.S. Leigh, R.M. Villahermosa, H.B. Gray, J.R. Winkler, Science 307 (2005) 99.
[103] O.S. Wenger, H.B. Gray, J.R. Winkler, Chimia 59 (2005) 94.
[104] O.S. Wenger, Chimia 61 (2007) 823.
[105] M. Hissler, W.B. Connick, D.K. Geiger, J.E. McGarrah, D. Lipa, R.J. Lachicotte, R. Eisenberg, Inorg. Chem. 39 (2000) 447.
[106] J.E. McGarrah, R. Eisenberg, Inorg. Chem. 42 (2003) 4355.
[107] J.E. McGarrah, Y.J. Kim, M. Hissler, R. Eisenberg, Inorg. Chem. 40 (2001) 4510.
[108] S. Chakraborty, T.J. Wadas, H. Hester, R. Schmehl, R. Eisenberg, Inorg. Chem. 44 (2005) 6865.
[109] C. Monnereau, J. Gomez, E. Blart, F. Odobel, S. Wallin, A. Fallberg, L. Hammarström, Inorg. Chem. 44 (2005) 4806.
[110] N.P. Redmore, I.V. Rubtsov, M.J. Therien, J. Am. Chem. Soc. 125 (2003) 8769.
[111] H. Imahori, K. Tamaki, D.M. Guldi, C.P. Luo, M. Fujitsuka, O. Ito, Y. Sakata, S. Fukuzumi, J. Am. Chem. Soc. 123 (2001) 2607.
[112] H. Imahori, D.M. Guldi, K. Tamaki, Y. Yoshida, C.P. Luo, Y. Sakata, S. Fukuzumi, J. Am. Chem. Soc. 123 (2001) 6617.
[113] H. Imahori, Y. Sekiguchi, Y. Kashiwagi, T. Sato, Y. Araki, O. Ito, H. Yamada, S. Fukuzumi, Chem. Eur. J. 10 (2004) 3184.
[114] D.M. Guldi, H. Imahori, K. Tamaki, Y. Kashiwagi, H. Yamada, Y. Sakata, S. Fukuzumi, J. Phys. Chem. A 108 (2004) 541.
[115] G. de la Torre, F. Giacalone, J.L. Segura, N. Martin, D.M. Guldi, Chem. Eur. J. 11 (2005) 1267.
[116] G. Kodis, P.A. Liddell, L. de la Garza, A.L. Moore, T.A. Moore, D. Gust, J. Mater. Chem. 12 (2002) 2100.
[117] P.A. Liddell, G. Kodis, D. Kuciauskas, J. Andreasson, A.L. Moore, T.A. Moore, D. Gust, Phys. Chem. Chem. Phys. 6 (2004) 5509.
[118] K. Kilså, J. Kajanus, A.N. Macpherson, J. Mårtensson, B. Albinsson, J. Am. Chem. Soc. 123 (2001) 3069.
[119] M.U. Winters, K. Pettersson, J. Mårtensson, B. Albinsson, Chem. Eur. J. 11 (2005) 562.
[120] K. Pettersson, J. Wiberg, T. Ljungdahl, J. Mårtensson, B. Albinsson, J. Phys. Chem. A 110 (2006) 319.
[121] J. Wiberg, L.J. Guo, K. Pettersson, D. Nilsson, T. Ljungdahl, J. Mårtensson, B. Albinsson, J. Am. Chem. Soc. 129 (2007) 155.
[122] M.U. Winters, E. Dahlstedt, H.E. Blades, C.J. Wilson, M.J. Frampton, H.L. Anderson, B. Albinsson, J. Am. Chem. Soc. 129 (2007) 4291.
[123] F.C. Grozema, C. Houarner-Rassin, P. Prins, L.D.A. Siebbeles, H.L. Anderson, J. Am. Chem. Soc. 129 (2007) 13370.
[124] S. Bhosale, A.L. Sisson, P. Talukdar, A. Fürstenberg, N. Banerji, E. Vauthey, G. Bollot, J. Mareda, C. Röger, F. Würthner, N. Sakai, S. Matile, Science 313 (2006) 84.